Islam M. Khattab   ORCID iD: 0000-0003-2370-0766

Ferulic acid is a putative surrender signal to stimulate programmed cell death in grapevines after infection with *Neofusicoccum parvum*

Islam M. Khattab[1,2,*], Jochen Fischer[3], Andrzej Kaźmierczak[4], Eckhard Thines[3] & Peter Nick[1]

[1] Molecular Cell Biology, Botanical Institute, Karlsruhe Institute of Technology, Fritz-Haber-Weg 4, 76131 Karlsruhe, Germany.

[2] Department of Horticulture, Faculty of Agriculture, Damanhour University, P.O. Box 22511 Damanhour, Egypt.

[3] Institut für Biotechnologie und Wirkstoff-Forschung gGmbH, Erwin-Schrödinger-Str. 56, 67663 Kaiserslautern, Germany

[4] Department of Cytophysiology, Institute of Experimental Biology, Faculty of Biology and Environmental Protection, University of Łódź, Pomorska 141/143, 90-236 Łódź, Poland

ORCID IDs:

0000-0003-2370-0766 (I.M.K); 0000-0002-0763-4175 (P.N);

Author for correspondence:

Islam M. Khattab

Email: islam.khattab@kit.edu

Total word count for the main body of the text after fulfilling the required edits by the reviewers in (introduction, methodology, results, and discussion) after two submissions; 8816

Introduction; 1742

Methodology; 2126

Results; 3104

Discussion; 1844

Nr. of main figures; 10 (in colour)

Nr. of supplementary files; 1 supplementary method, 7 supplementary figures (in colour) and 1 supplementary table.

Summary

Apoplectic breakdown from Grapevines Trunk Diseases (GTDs) has become a serious challenge to viticulture in consequence to drought stress. We hypothesise that fungal aggressiveness is controlled by a chemical communication between host and colonising fungus. We introduce the new concept of a "plant surrender signal" accumulating in host plants under stress and facilitating the aggressive behaviour of the strain *Neofusicoccum parvum* (Bt-67) causing *Botryosphaeriaceae*-related dieback in grapevines. Using a cell-based experimental system (*Vitis* cells) and bioactivity-guided fractionation, we identify *trans*-ferulic acid, a monolignol precursor, as "surrender signal". We show that this signal specifically activates secretion of the fungal phytotoxin Fusicoccin A aglycone. We show further that this phytotoxin, mediated by 14-3-3 proteins, activates programmed cell death in *Vitis* cells. We arrive at a model showing a chemical communication facilitating fusicoccin A secretion that drives necrotrophic behaviour during *Botryosphaeriaceae-Vitis* interaction through trans-ferulic acid. We thus hypothesise that a channeling of the phenylpropanoid pathway from this lignin precursor to the trans-resveratrol phytoalexin could be a target for future therapy.

One sentence summary
This study identified for the first time a new level of plant-pathogen crosstalk, so-called "plant surrender signal", which triggers the endophyte transition from asymptomatic commensalism to a necrotrophic lifestyle killing the vine "*Vitis vinifera*" in a few days

Keywords: Grapevines, *Neofusicoccum parvum*, programmed cell death, Fusicoccin A, Plant surrender signal, Ferulic acid

Introduction

Concomitantly with the current climate change, *Botryosphaeriaceae*-related Dieback turned into a progressively devastating threat for viticulture. Around a decade ago, the economic damage by Grapevine Trunk Diseases (GTDs) was estimated to exceed 1500 Million US$ per year (Hofstetter *et al*., 2012), already in 2016 alone for France yield was reduced by 25% corresponding to around 5000 Million US$ (https://www.maladie-du-bois-vigne.fr). The interaction of *Botryosphaeriaceae* with their grapevine hosts is very complex. The infection process displays two phases – a latent phase linked with reduced vigour of the host that can last very long, and an apoplectic phase during which the host dies off within a few days (Slippers & Wingfield, 2007) as shown in **Fig. S1**. To which extent the onset of apoplexy is linked with a switch towards necrotrophy, remains to be elucidated. This lifestyle is typical of Grapevine Trunk Diseases (GTDs) and differs from other pathogens, because it does not meet Koch's postulates defining the criteria for a causative relationship between microbial pathogens and their hosts (Loeffler F. 1884). In case of wood decaying diseases, there is no strict link between the presence of the microbe and the appearance of disease symptoms. During the endophytic phase this link seems to be absent, it is a change of fungal behaviour (not the presence of the microbe) that causes apoplexy (**Fig. 1**).

GTDs have always been present in Europe. In fact, the pathogenicity of wood decaying diseases has been a very ancient phenomenon in vineyards. The first report, written in Arabic, in the book *Kitab Al-Felaha* by the Andalusian Scientist *Ibn Al-Awam* dates back to the twelfth century, and, only two centuries later, a Latin description was given in *Opus Ruralium Commodorum* by the scientist *Pietro de' Crescenzi* from Bologna (Mugnai *et al*., 1999). Nevertheless, the more common outbreak of the symptoms correlates with climate change (Slippers & Wingfield, 2007; Galarneau *et al*., 2019). Although GTD has been manifest for a long time, we know very little about the molecular mechanisms that provoke a harmless endophyte to turn into a dangerous, toxin-producing killer. Although the impact of plant-pathogen crosstalk in the context of GTDs is clear, we are still far from understanding this crosstalk.

Botryosphaeriaceae related Dieback occurs all over the world and about 21 species of the *Botryosphaeriaceae* associate with dieback in grapevines (Carlucci *et al.*, 2015). The species *Neofusicoccum parvum* has served as experimental model to study *Botryosphaeriaceae* related Dieback as one of the most aggressive fungal strains (Úrbez-Torres & Gubler, 2009; Stempien *et al*., 2017).

Visible symptoms appear usually during advanced stages of the disease. These include cankers in the perennial wood, dead spurs and buds, as well as discolouration of leaves, although these fungi never colonise the leaves of infected grapevines (Mugnai *et al*., 1999; Úrbez-Torres, 2011). The fungus initiates colonisation through wounded wood tissues, usually in the context of pruning (Djoukeng *et al.,* 2009; Úrbez-Torres, 2011). Anatomical investigations showed that the fungus spreads through xylem vessels or parenchymatic rays (Gómez *et al.*, 2016; Massonnet *et al.,* 2017; Khattab *et al*., 2021).

Since plants are sessile organisms, efficient immunity responses are mandatory to cope with attack by invading organisms. Therefore, plant immunity comes in two levels (for review see Jones & Dangl, 2006; Chuberre *et al*., 2018). First, a broadband basal immunity acts against entire classes of microbes. Second, a specific immunity, often acting against particular strains of a given pathogen, but not always accompanied by hypersensitive cell death, where infected cells commit to suicide for the sake of the other cells.

Vitis responds to a *Botryosphaeriaceae* infection by activation of genes for phytoalexin biosynthesis and by accumulation of the respective compounds. However, due to feedback from metabolites to gene activity both responses are not necessarily parallel. For instance, in several studies, the induction of phytoalexin-related transcripts was not correlated with the degree of susceptibility (Massonnet et al., 2017; Leal et al., 2021; Labois et al., 2020; Khattab et al., 2021). High transcript accumulation was, here, often an indicator for a higher stress level, i.e., for susceptibility. Inoculation of *Vitis* plants with *N. parvum* caused a strong decrease in the primary metabolites like sugars, followed by the accumulation of secondary metabolites, such as stilbenes (Labois *et al*., 2020). This indicates that host metabolism re-partitions towards defence compounds. However, this metabolic re-partitioning does not necessarily restrict fungal spread. A comparative study with

different chemotypes of *V. sylvestris* demonstrated that the higher steady-state transcripts of stilbene synthase genes do not necessarily mean corresponding increases of secondary metabolite abundance. Nevertheless, the efficient containment of the fungus correlates with the local accumulation of specific bioactive phytoalexins, such as viniferine trimers, while glycosylated stilbene species seemed to be irrelevant (Khattab *et al.,* 2021).

With respect to the fungal counteraction, *Botryosphaeriaceae* related Dieback correlates with the secretion of phytotoxic polyketides. Although these compounds seem to be recognised by the host, leading to a defence response, they have to be seen rather as virulence factors, not as elicitors. While it is conceivable that these compounds act as phytotoxins that kill the host cell, before it is able to deploy a defence response, they might also hijack signalling in the host to support successful invasion. For instance, such signals might induce Programmed Cell Death, which is an efficient defence reaction in the context of a biotrophic pathogen, but counterproductive, if the host cell deals with a necrotrophic pathogen. The fact that the entire secretome of *Botryosphaeriaceae* caused more necrosis in a Chardonnay callus system (Stempien et al., 2017) as compared to the polyketide fraction alone, indicates that virulence factors other than polyketides might act as amplifiers. The bioactivity seems to be species-dependent, since secretions of *N. parvum* were found to be more aggressive than *Diplodia seriata* (Ramírez-Suero *et al.*, 2014). Indications for a signalling effect come, for instance, from findings that the polyketide terremutin secreted by *N. parvum* not only causes leaf necrosis but also triggers genes regulating flavonoid biosynthesis pathway (Abou-Mansour *et al.*, 2015). The toxic polyketide neoanthraquinone causing drastic shrivelling in *Vitis* leaves is secreted by the related species *N. luteum* (Pescitelli *et al.*, 2020). A widespread compound found across the entire *Botryosphaeriacea* family is mellein or derivatives thereof, found, for instance, in many *Neofusicoccum* members in Australia and Europe (Andolfi et al., 2011). For instance, Reveglia et al (2021) have shown that the amount of (R)-mellein detected in infected woods was correlated with the amount of the detected fungal DNA. Also mellein was described as a virulence factor of *Botryosphaeriaceae* related Dieback, thus increasing disease severity (Trotel-Aziz et al. 2022), although given alone it exerts only a low activity on grapevine leaf discs (Masi et al., 2018).

Botryosphaeria dieback of the host plant is not only correlated to secreted fungal phytotoxins which accumulate in the foliar system following the transpiration stream, but also results from the hydraulic failure by tyloses and gelous depositions in the infected vessels (Bortolami *et al*., 2019; Claverie et al., 2020). For grapevine wilts caused by *Phaeomoniella*, wider xylem vessels were proposed to be linked with susceptibility for apoplectic breakdown, which was linked with a stronger tendency for tyloses and gel pockets allowing the fungus to escape from occluded vessels (Pouzoulet *et al.*, 2017). However, during a comparative study for the spread of *N. parvum*, fungal spread did not correlate with vessel diameter, but rather depended on differential channelling of the stilbene pathway (Khattab *et al.,* 2021). Moreover, susceptibility was reported to correlate with the abundance of transcripts for key genes of lignin biosynthesis, like *Caffeic acid O-methyltransferase* which catalyses the conversion of trans-ferulic acid from caffeic acid (Umezawa, 2010) (https://www.uniprot.org/uniprot/Q06509), consistent with the finding that a higher lignin content represents a hallmark of susceptibility (Khattab *et al.,* 2021).

After a long biotrophic phase, *N. parvum* turns to necrotrophy leading to decreased vigour of the host, and eventually apoplexy. The molecular mechanisms behind this switch in the lifestyle of this "hemibiotrophic" pathogen are still elusive. However, the outbreak of GTD seems to be strongly correlated to drought stress, accentuated in consequence of global warming, which holds true for both, the Esca syndrome (Lima *et al,* 2017), and *Botryosphaeriaceae*-related Dieback (Galarneau *et al.*, 2019). While the fungus needs to be present to observe symptoms of the disease, it is not a sufficient condition to trigger apoplexy. Since apoplexy is a conditional phenomenon, it might result from altered chemical communication between plant and fungus (**Fig. 1**). Compared to true hemibiotrophs, *Botryosphaeriaceae* fungi seem to represent an evolutionarily ancestral stage of necrotrophy, since they can live as saprotrophs in the wood over many years, before but turning into necrotrophs and, in the terminal stage, inducing apoplexy. Prior to the actual apoplexy, during the so-called pre-critical phase, the fungus colonises the wood as endophyte, using cell-wall degrading enzymes, and the host plant responds by synthesis of phytoalexins. Under climate-borne stress, the fungus leaves the pre-critical phase culminating in apoplectic breakdown of the host. The weakened defence response of the host, possibly along with the metabolic changes in the plant evoked by the abiotic stress, allow the fungus

to sense a future limitation of resources, which alters the fungal strategy. In response to these metabolic changes in the host changes, the fungus releases distinct polyketides acting virulence factors for the necrotrophic, terminal phase. Thus, it is the metabolic state of the plant seems to condition the aggressiveness of the pathogen.

In the present study, we test the hypothesis that the *Botryosphaeriaceae*-related Dieback in grapevines results from a chemical communication between host and pathogen. We used *N. parvum* Bt-67, as one of the most aggressive and virulent fungal strains causing this disease (Guan *et al.*, 2016; Stempien *et al.*, 2017). We developed a cell-based experimental system to study plant-fungal interaction *in vitro*. This experimental system allowed us to screen candidate plant compounds that accumulate under drought stress and can trigger the release of fungal compounds with the strongest phytotoxic activity. We first identified the lignin precursor ferulic acid as specific and efficient activator for the release of fungal phytotoxins. Using bioactivity-guided fractionation, we were then able to identify a Fusicoccin A (FCA) aglycone as *bona-fide* candidate for the strong phytotoxic effect. In the third part of the study, we analysed the mode of action of FCA and found that this compound induced programmed cell death in grapevine cells. Our study aims to show that in the context of host-hemibiotrophic interaction under external stress, the fungus benefits of the plant responses to complete the infectious process.

Materials and Methods:

Plant and fungal materials

The used fungal strain in the study, *Neofusicoccum parvum Bt-67*, was kindly provided by Laboratoire Vigne Biotechnologies et Environnement, Université de Haute-Alsace, France and isolated by Instituto Superior de Agronomia, Universidade de Lisbona, Portugal (Reis et al., 2016; Stempien *et al.,* 2017). We conducted the experiments with the grapevine suspension line Vrup-TuB6-GFP, deriving from *Vitis rupestris,* and expressing a N-terminal fusion of GFP with ß-tubulin 6 (Guan *et al.*, 2015). The response of actin filaments was followed using a cell line in *Vitis vinifera* cv. Chardonnay expressing a florescent fimbrin actin-binding domain 2 (*At*FABD2)-GFP (Akaberi *et al.,* 2018). Also, two transgenic lines in tobacco (*Nicotiana tabacum* L. cv. 'Bright-Yellow 2' overexpressing *V. rupestris* Metacaspases 2 and 5 were used

along with their non-transformed wild type (Gong *et al.*, 2019). All cells were subcultured in weekly intervals into Murashige and Skoog medium. The transgenic lines remained under selective pressure by the appropriate antibiotics. All experiments were conducted with cells that were not cycling, either because they had already entered the expansion phase (four days post subculture for the grapevine cell lines) or were still in the lag phase prior to the first division (one day post subculture of tobacco BY-2 cells).

Screening the effect of monolignol precursors on *N. parvum* aggressiveness

To probe whether the monolignol precursors cinnamic acid, *p*-coumaric acid, caffeic acid, and *trans*-ferulic acid can induce *N. parvum* to secrete phytotoxic compounds, fungal mycelia were fermented with different concentrations (0.5, 1, 1.5 mM) for each of the mentioned monolignol precursors. Fungal mycelia, grown for 2 weeks on Potato Dextrose Agar, PDA (Sigma-Aldrich, Deisenhofen), were cultivated with the respective compound in 250 ml of 20 $g^.L^{-1}$ malt extract medium (Carl Roth GmbH, Karlsruhe, Germany), pH 5.3 for two additional weeks. After sterile filtration through a 0.22-µm PVDF membrane (Carl Roth GmbH, Karlsruhe, Germany), the culture filtrate was added to the Vrup-TuB6 cells (35 µl. filtrate / ml. cell suspension) to test for a potential phytotoxic effect.

To explore whether phytotoxic compounds might be retained inside the hyphae without being secreted, we extracted fungal metabolites, either from medium or mycelia, after 24 h fermentation with the respective precursor after the fungus consumed entirely the sugar, which was checked with a Diabur 5000 test strip (Roche, Basel; Switzerland).

Extraction of fungal metabolites, HPLC and HPLC-MS analysis for the toxic fraction

The fungus was cultured in 20 L Yeast Malt Glucose medium (yielding from the culture filtrate about 7.2 g of a crude extract after *trans*-ferulic acid supplement) as explained in **S. Method 1**. Phases of different hydrophobicity (0, 10, 20, 30, 40, 50, 60, 70, 80, 90, 100% MeCN) were then tested for their bioactivity in the *Vitis* cell culture system. To identify the fungal phytotoxin released in response to *trans*-ferulic acid, the most toxic phase was re-analysed by a HPLC-MS (Series 1200, Agilent,

Waldbronn, Germany) equipped with an UV-DAD and a coupled LC/MSD Trap APCI-mass spectrometer with positive and negative polarisation as described by Buckel *et al*. (2017). For the mass spectrum of the derived molecules as well as their HPLC-MS analysis see **S. Fig. 4.** The HPLC-MS analysis of the fraction with the strongest phytotoxicity upon *Vitis* cells identified a Fusicoccin A aglycone. The Fusicoccin A signal was verified by a Fusicoccin A standard, which is part of the IBWF database (CAS 20108-30-9; sc-200754) bought at Santa Cruz Biotechnology, Inc.

Mapping the deathly signalling pathway triggered by FCA.

After identifying FCA as fungal phytotoxin, the cellular responses to a synthetic FCA (Santa Cruz Biotechnology, Heidelberg, Germany) were analysed. We used two concentrations of FCA (6 and 12 μM) to probe the responses of *Vitis* cells, using the line Vrup-TuB6-GFP. To get insight into the cellular events involved in this response, a pharmacological strategy was employed as follows:

Blocking the FCA receptor, a 14-3-3 protein.

Fusicoccin receptors were blocked using BV02 (Sigma-Alrich, Germany Stevers *et al.,* 2018) which inhibits 14-3-3 proteins docking sites as shown in the experimental scheme (**Fig. 6a**). Here, Vrup-Tub6-GFP cells were incubated for 60 min first with 5 μM of BV02, diluted in 100 μM DMSO, prior to FCA treatment.

Inhibiting Respiratory burst Oxygen Homolog (RbOH)

Prior to FCA treatment, *Vitis* cells were pre-treated for 60 min with 1 μM of Diphenyleneiodonium chloride (DPI; Sigma-Aldrich, Germany), diluted in 100 μM DMSO, which binds to NAD(P)H oxidases in the plasma membrane as shown in the synthetic scheme **(Fig. 6e)**, inhibiting reactive oxygen species (ROS) synthesis in the apoplast (Chang *et al*., 2011).

Measurement of extracellular pH

Changes in the extracellular pH can be used to monitor cellular responses in a non-invasive manner. For instance, activation of plasma membrane ATPases will lead to acidification, while defence-related opening of Ca^{+2} influx channels, by co-import, will lead to alkalinisation. This allows to follow early responses to extracellular

signals such as pathogenic mobile polyketides such as Mellein, and Fusicoccin (Huang, et al, 2014; Kesten et al., 2019; Guan et al., 2020). Therefore, we followed changes in the extracellular pH in Vrup-TuB6-GFP cells by pH meter (Schott handylab, pH12) and recorded by a digital memory recorder displaying the pH at 1-second intervals as detailed in Qiao *et al.* (2010). To test effect of blocking 14-3-3 proteins as FCA receptors on ATPases activity, cells were pre-incubated with 5 µM of the 14-3-3 blocker for 45 min, and then treated by FCA (6 µM).

Superoxide [O_2-] detection

ROS play a dual role in biotic stress signalling. They can activate basal defence, or they can induce programmed cell death depending on their temporal relationship with calcium influx (Chang & Nick, 2012). Therefore, we estimated the intracellular superoxide accumulation in *Vitis* cells by the 0.1% (w/v) Nitroblue Tetrazolium (NBT) assay as described in Steffens & Sauter (2009) and Pietrowska *et al.* (2014) with modifications. After filtering suspension cells from the culture medium, we incubated the *Vitis* cells in NBT for 1 h under aseptic conditions before washing in phosphate buffer prior to observation by bright-field microscopy (Axioskop, Zeiss). Cells accumulating superoxide appeared in blue colour. The frequency of stained cells served as readout for superoxide accumulation, scoring 600 individual cells for each of three biological replicates of the respective time-point.

Live-cell imaging of the cytoskeleton

Since cytoskeletal integrity plays a key role in stress signalling in response to variable pathogen polyketides (Qiao et al., 2010; Guan et al., 2020), we followed the response of the cytoskeleton to FCA using two GFP-tagged marker cell lines. For visualisation of microtubules, we employed the marker line Vrup-TuB6 expressing *At*TUB6-GFP (Guan *et al.*, 2015). We observed actin filaments in the marker line from *V. vinifera* cv. 'Chardonnay' expressing Vv-*At*FABD2-GFP (Akaberi *et al.*, 2018), since attempts to engineer an actin-marker cell line in the background of *V. rupestris* have not been successful. The cytoskeletal response was captured by spinning disc confocal microscopy with an AxioObserver Z1 (Zeiss, Jena, Germany) microscope, equipped with a spinning-disc device (YOKOGAWA CSU-X1 5000), and 488 nm emission light from an Ar-Kr laser (Wang & Nick 2017). We collected confocal z-stacks,

processed them by the ZEN software (Zeiss, Oberkochen), and exported them as TIFF format.

To quantify the width of actin filament, as readout for actin bundling which acts as an early hallmark for hypersensitive cell death signalling (Chang et al, 2015; Smertenko & Franklin-Tong, 2011), we transformed the cells of interest into binary images, adjusting the threshold with the B/W option of the ImageJ freeware (https://imagej.nih.gov/ij). Using analyze particles tool, actin filaments were selected automatically. We filtered out random signals by setting the detection threshold to 10 square pixels and using the fit ellipse command to fit the detected particles and to quantify the short ellipse axis as readout for filament width. The integrity of cortical microtubules was estimated based on the strategy in Schwarzerová, *et al.* (2002). We collected four intensity profiles along the long axis of the cell in equal spacing over the cross axis and using a line width of 25 pixels according to modifications described in Guan *et al*. (2020). For both, microtubule or actin filament quantification, twenty-five individual cells were scored for each treatment representing 4 independent biological replicates.

modulation of the cytoskeleton

Cytoskeletal organisation was modulated either by stabilisation or elimination to investigate its role in FCA signalling pathway. To assess the role of microtubuleson the response to FCA, Vrup-TuB6-GFP were either pre-treated with 10 µM of Taxol (Sigma-Aldrich, Germany), which stabilises microtubules, or with 10 µM of Oryzalin, eliminating microtubules (Sigma-Aldrich, Germany) for 30 min, before adding FCA as displayed in the experimental scheme (**Fig. 7a**). To assess the role of the actin filaments, cv. Chardonnay expressing *At*FABD2-GFP marker were pre-treated with 2 µM of the actin-eliminating compound Latrunculin B (Sigma-Aldrich, Deisenhofen, Germany) for 1 hr prior to FCA treatment as shown in (**Fig. 8a**).

RNA extraction and qRT-PCR

V. rupestris (*At*TUB6-GFP) cells were collected, and immediately frozen in liquid nitrogen. We extracted total RNA with the RNA Purification Kit (Roboklon, Berlin, Germany). We used 1 µg of total RNA as template for cDNA synthesis, pre-incubating with oligo (dT) primers, followed by reverse transcription with M-MuLV enzyme (New England Biolabs; Frankfurt, Germany) in presence of RNase inhibitor.

We monitored transcripts of defence-related genes regulating either cell-death signalling or phenylpropanoid pathway and hormone signalling by qRT-PCR using CFX-PCR System (Bio-Rad, München; Germany) as described in Svyatyna *et al.* (2014). The housekeeping gene, *EF-1α*, served to calculate the steady-state transcripts of target genes using the $2^{-\Delta\Delta Ct}$ method (Livak and Schmittgen, 2001). For details of primer sequences, and accession numbers of target genes see **Table S1**.

Cell death assays

To characterise the type of cell death, we incubated Vrup-TuB6-GFP cells for two min with a double staining solution, containing Acridine Orange, AO (100 µg.mL^{-1}) and Ethidium Bromide, EB (100 µg.mL^{-1}) (Byczkowska *et al.*, 2013). The stained cells were analysed by fluorescence microscopy (Diaplan, Leitz) upon excitation in the blue (filter set I3, excitation 450–490 nm, beam splitter 510 nm) recording emission above 515 nm and digital image acquisition (Leica DFC 500 and Leica Application Suite, v4). Living cells exclude EB and appear green. Cells in stage I show penetration of EB only into the cytoplasm, giving greenish-yellow to yellow nuclei. Cells in stage II show bright orange nuclei, because EB crosses the nuclear envelope. Dead cells lose the AO after the breakdown of plasma membrane, while EB remains sequestered at the DNA, displaying red nuclei. Frequency distributions represent 300-400 individual cells collected from three independent experimental series.

In addition, we used the Evans Blue Dye Assay (Gaff and Okong'o-Ogola, 1971) which labels dead cells blue to a loss of membrane integrity. We stained the *Vitis* cells with 2.5 % Evans blue (Sigma Aldrich, Germany) for 3 min, and then washed twice with distilled water to remove unbound dye. Mortality scores represent populations of at least 1000 individual cells for each biological replicate of the respective treatment.

***In-planta* infection assay and drought stress.**

To test the effect of drought stress on disease outbreak, we followed disease development in infected grapevines under two water regimes in the variety *V. vinifera* cv. 'Augster Weiss' (a male sterile variety often used for genetic introgression, in preparation of future research on resistance breeding), rather than *V. rupestris*, which had been used for the cellular studies, because, here, a fluorescent microtubule marker

line was available. After pre-cultivation of woodcuttings for 3 months in pots in the greenhouse, we infected healthy and homogenously grown individuals with *N. parvum* Bt-67 mycelia according to Khattab *et al.* (2021), and directly subdivided into two experimental sets. One set was well irrigated in 5 days/week and served as control, while the other set developed under constrained irrigation (watering only once weekly). Each set consisted of infected plants and the respective mock control.

Fungal colonisation and lignin accumulation

We evaluated the result 30 days later for wood necrosis and lignin content according to Khattab *et al.* (2021) in the infection site, but also at the lower and upper margin of the internode (3 cm below or above the infection site). To evaluate the spread of the fungus through the internodes we quantified the fungal DNA after extracting genomic DNA from the wood as described in Cota-Sánchez, *et al.* (2006). We measured the abundance of fungal DNA by qPCR using 25 ng of DNA template, 1 unit of *Taq Polymerase* (England Biolabs; Frankfurt, Germany), and specific ITS primers, which bind exclusively to *Botryosphaeriaceae* DNA (Ridgway *et al.,* 2011). For the details of primers and the PCR conditions refer to **Table S1**. The abundance of the fungal DNA was evaluated using a calibration curve (Flubacher 2021), which was calculated based on a dilution series of transformed plasmid DNA amplified by TA cloning in the pGEM®-T Easy vector (ThermoFisher) according to the protocol of the producer.

Results

Drought stress promotes infection development and lignin accumulation.

Since drought, as accentuated by climate change, seems to promote disease outbreak, we tested whether restricted irrigation would accentuate the grapevines response to infection with *N. parvum*. The degree of imposed drought stress was sufficient to induce significant symptoms i.e., reduced growth and partial leaf discoloration (**Fig. 2a**). The wood necrosis due to *N. parvum* Bt-67 infection (**Fig. 2b**, *NP*) was almost twice in the plants under drought stress. To check, whether the increase in symptomatic wood under drought stress is related to fungal development, the fungal DNA abundance was quantified one month after inoculation using a *Botryosphaeriaceae* specific internal transcribed spacer (*its*) for detection (**Method. S1: Fig. S2**). In fact, we observed that the abundance of fungal DNA was more than

twofold increased under drought stress as compared to control condition in the inoculation site itself, while the two sites 3 cm below or above did not differ.

We also observed that infection induced a significant lignin accumulation. Since drought induced somewhat more lignin (**Fig. 2c, W**), the lignin content after infection (**Fig. 2c**, **NP**) was slightly, but significantly higher than the value in the infected control. However, there is no indication for a synergistic interaction between infection and drought with respect to lignin deposition, the two factors seemed to act additively.

In response to ferulic acid, *N. parvum* secretes a FCA aglycone.

Since *N. parvum* aggressiveness depends on plant-derived factors that associate with the stress level of the plant, we tested different monolignol precursors for their ability to elicit the release of fungal factors with toxicity on *Vitis* cells (**Fig. 2d, e**). When we fermented the mycelia in presence of cinnamic acid, and added the culture-filtrate to *Vitis* cells, these cells displayed a mortality that was significantly lower than the mortality in response to filtrate from untreated mycelium. In a similar manner, supplementation of both, *p*-coumaric acid and caffeic acid, reduced the toxicity of the fungal culture-filtrate reaching to the residual mortality levels seen in untreated cells (**Fig. 2d**), irrespective the precursor concentration (**Fig. S3**). However, fermenting the mycelia with ferulic acid, a low concentration of 0.5 mM, boosted the toxicity of the culture-filtrate, increasing the mortality levels from 32% to 55% (**Fig. 2e**). We observed as well that the mycelia switched to the sexual cycle as evident from excessive spore release when ferulic acid was present in the medium. Asking further whether the difference between ferulic acid and its precursor coumaric acid was due to differences in secretion or to differences in accumulation. To address this, we separated the fungal metabolites secreted to the medium from those remaining inside mycelia. Mycelium extract led to similar mortality rates in the target cells, no matter, whether the mycelium had grown untreated or in presence of *p*-coumaric acid or ferulic acid (**Fig. 2f**). On the other hand, the culture-filtrates from the very same cells induced a different mortality: Fermentation in presence of *p*-coumaric acid produced less phytotoxic culture-filtrate than that from *N. parvum* alone, while fermentation with ferulic acid caused higher mortality than the control culture-filtrate of *N. parvum* (**Fig. 2f**). This indicates that *p*-coumaric acid and ferulic acid do not differ with

respect to their effect on phytotoxin biosynthesis, but with respect to phytotoxin secretion.

To identify the compound responsible for the phytotoxicity, we separated the fungal metabolites based on the hydrophobicity. Hereby, specific peaks only appeared after ferulic treatment and increased, when the hydrophobicity (% MeCN) increased (**Fig. 3a**). These peaks were absent, when the fractions originated from fungi fermented in the absence of ferulic acid (**Fig. S4**). These peaks differed with respect to their hydrophobicity. For instance, a vanillic acid-like compound (**Fig. 3a**, orange box) increased first with rising concentrations of MeCN but was absent in the most hydrophobic fraction (100% MeCN), while a mellein-like compound increased up to 50% MeCN but lacked in 75% and 100% MeCN fractions (**Fig. 3a**, blue box). One peak (**Fig. 3a**, red box, retention time 4,79 min) was prominent, because it increased progressively with increasing the hydrophobicity of the extraction. This peak qualified as bioactive candidate, because the phytotoxicity of the fungal metabolites produced in response to ferulic acid increased with the hydrophobicity of the fraction (**Fig. 3b**), with a very strong correlation (R= 0.99). In fact, when we plotted the induced mortality over the area for the peak at retention time 4.79 min (**Fig. 3a**, red box), we found a clear saturation curve with a high correlation of R=0.9 (**Fig. 3c**).

Consequently, the most hydrophobic phase was selected for further sub-fractionation by LC and characterisation by MS. For the absorption and mass spectra of these sub-fractions refer to **Fig. S5**. These fractions from LC were then further tested for their ability to induce mortality in the *Vitis* cells (**Fig. 2d**). Here, the highest bioactivity dwelled in fractions B1 and B2, respectively (**Fig. 2d**). HPLC-MS analysis identified the bioactive compound in the most toxic, fraction B1, as Fusicoccin A without sugar moiety, FCA aglycone (**Fig. 3e**). In the following, we tried to elucidate the mode of action of FCA.

FCA induces autolysis in grapevine cells.

To get insight into the quality of mortality induced by FCA, we treated *V. rupestris*, *At*TUB6-GFP cells with either 6 or 12 μM FCA (**Fig. 4a**) and followed the progression of cell death using double staining with AO (membrane permeable) and EB (membrane impermeable, DNA binding) to classify the dying cells into different

stages as described in methodology. In response to FCA, the frequency of cells in stage I and dead cells (**Fig. 4f**) became more abundant. This progression was accelerated for the higher concentration of FCA. The lower dose of 6 μM FCA required 6 h to cause similar mortality as seen for 12 μM FCA at 3 hrs treatment. Roughly, the velocity of the response increased proportionally with the concentration. The frequency of cells in stage II was low and mostly constant through all time-points. Interestingly, this steady-state level was higher for 6μM FCA (around 10-15%) comparing to the higher dose (around 5-10%). Together with the low incidence, this fact indicates that stage II is short-lived. A cell that is losing the tightness of the nuclear envelope against EB is doomed to timely death. When the response to FCA is speeding up, this will also reduce the steady-state level of stage II.

In addition, this double staining assay allowed to observe transitional stages displaying cytological hallmarks of autolytic cell death. For instance, transition to stage I was heralded by chromatin condensation (**Fig. 4c**), while progression through stage I was accompanied by the formation of lytic vacuoles in the cytoplasm of dying cells (**Fig. 4d, e**). In the terminal stage, the nuclei were red, while the cytoplasmic signals observed in dying cells, vanished (**Fig. 4 c, d, e**).

To test, whether the response of grapevine cells would be reflected in a corresponding response of grapevine tissues, we administered FCA (9 μM) to leaves through the petiole. In fact, we saw that FCA induced severe leaf necrosis when scored 20 h after the onset of the treatment (**Fig. S6**). Thus, the death response to FCA also proceeds in cells that are embedded in a tissue context.

The response to FCA recapitulates cell-death related defence.

To map the signalling deployed by FCA, we used a concentration 6 μM. We observed a fast drop of extracellular pH, as it would be expected from activation of plasma-membrane (PM) proton ATPase. This acidification reached around -0.2 units within 30 min, kept a plateau for another 20 min and then underwent a second round of acidification reaching to -0.3 units at 90 min after addition of FCA (**Fig. 5a**).

To measure RbOH activity in response to FCA, we visualised superoxide by NBT staining. The proportion of cells staining positive for superoxide increased rapidly to around 25% within 1 h after addition of FCA (**Fig. 5b**), with significant increases over

the control level already at the first measurable time-point (10 min). After the peak at 60 min, the frequency of NBT positive cells dropped but remained elevated (three-fold of control cells). This drop might be linked with a loss of membrane integrity as found already substantial in the AO/EB staining (**Fig. 4a**).

To get insight into FCA signalling pathway, we followed steady-state transcripts levels of potential stress-marker genes in response to FCA, probing 1, 3 and 6 h (**Fig. 5c**). As markers for superoxide scavenging. The transcripts of *Superoxide Dismutase* genes (*MnSOD1* and *CuSOD2*) showed a rapid and steady induction, albeit to a mild extent. Also, *CuSOD1* displayed mild induction of transcripts only transiently, at 3 h by FCA. We also tested two metacaspases genes, *MC2* and *MC5*, that had been identified as markers for hypersensitive response in the *Vitis-Plasmopara* pathosystem (Gong *et al.*, 2019). Both meta-caspase transcripts were rapidly (within 1 h) upregulated by FCA but differed subsequently. While *MC5* declined later, the level of *MC2* transcripts continued to rise to reach a peak of more than 5-fold after 3 h.

The phenylpropanoid pathway gives rise to both monolignols (i.e., the substrate of the fungus) and to stilbenes (i.e., the central phytoalexin in grapevine). The transcripts of *PAL*, the first committed enzyme of the phenylpropanoid pathway was rapidly and massively (>30-fold) induced by FCA (**Fig. 5d**). Likewise, stilbene-biosynthesis transcripts accumulated significantly (10 to 20-fold) within 1 h, especially *STS27* and *STS47*. In contrast, the lignin biosynthesis genes, *CAOMT* and *CAD* did not show any notable induction.

In addition, FCA-challenged cells accumulated more transcripts of specific *JAZ* genes (*JAZ1* and *JAZ9*) (**Fig. 5d**). This indicates activation of jasmonate signalling as a hallmark of basal defence. To probe the salicylic signalling pathway, *NPR1* gene was slightly induced. Also, we observed a minor (1.6-fold) induction of *PR10*, while *PR1* was clearly upregulated (~6-fold).

This analysis shows that FCA induces a rapid extracellular acidification (probably by activating PM-ATPases), and a rapid increase of superoxide (possibly by activating RbOH). This is followed by rapid and massive induction of phytoalexin synthesis transcripts, and phytohormonal signalling (jasmonate pathway and salicylic-acid pathway). In parallel, transcripts for metacaspases involved in hypersensitive cell

death are induced. FCA is, thus, mimicking several aspects of a cell-death response as normally observed in response to pathogen attack.

FCA triggered PCD requires the activity of 14-3-3 proteins.

The activation of PM ATPases by FCA depends on anchoring 14-3-3 proteins. We asked, therefore, whether blocking 14-3-3 proteins by specific inhibitor BV02 (Stevers *et al.*, 2018) would not only inhibit proton ATPase activity, but also the signalling culminating in PCD. We observed that pre-treatment with BV02 inhibited extracellular acidification in response to FCA (**Fig. 6b**), demonstrating that the inhibitor was active. Pre-treatment with BV02 also modulated the transcript levels of stress-marker genes elicited by FCA (**Fig. 6c**). While the induction of transcripts for *JAZ1* by FCA was not altered by pre-treatment with BV02, the *STS27* and *STS47* by FCA became clearly amplified ($P<0.001$). On the other hand, the observed induction of *PAL* and *PR1* by FCA was significantly quelled ($P<0.001$). Likewise, the induction of metacaspases (*MC2* and *MC5*) by FCA was mitigated ($P<0.05$ and $P<0.001$, respectively).

Furthermore, blocking 14-3-3 protein activity by BV02 reduced strongly the mortality from 30% (FCA alone) to 16% for FCA administered after pre-treatment with BV02 (**Fig. 6d**). Since the mortality induced by BV02 alone was around 20%, this low mortality meant that BV02 completely eliminated the mortality induced by FCA.

Blocking apoplastic oxidative burst modulates FCA signalling.

The activation of defence-related PCD is linked with apoplastic oxidative burst originating from RbOH, we tested, whether the FCA signalling can be disrupted by pre-treatment with RbOH inhibitor (DPI). In fact, DPI significantly modulated the response to FCA. For instance, pre-treatment with DPI significantly reduced the superoxide production in response to FCA by a factor of two (**Fig. 6f**). This was also reflected on the transcript levels for stress-marker genes, albeit in different direction, depending on the gene (**Fig. 6g**). Transcripts of the basal defence genes *JAZ1, STS27,* and *STS47* were induced by DPI. Likewise, the induction by FCA was more pronounced in presence of DPI. The situation for *PAL* was different. Here, DPI alone induced *PAL* transcripts by about 10-fold. However, the induction, by FCA plus DPI, was declined to 50% of the level induced by FCA alone. A similar inhibition was

observed for the transcripts of *PR1* and *MC5* with significant levels *P*<0.001 and *P*<0.01, respectively. In addition, the induction of *MC2*, was mildly (but not significantly) inhibited. It should be mentioned that these three transcripts (*PR1*, *MC2*, *MC5*) associated with cell-death related defence (Chang and Nick, 2012; Gong *et al.*, 2019) were not induced by DPI alone (contrasting with *JAZ1*, *STS27*, *STS47*, and *PAL* that are associated with basal immunity). As to test, whether suppressing the FCA responses of *PR1*, *MC2* and *MC5* would result in a suppression of the cell death, we observed that inhibiting RbOH with DPI prior to FCA treatment significantly reduced the mortality (**Fig. 6h**) to the level seen for DPI treatment alone.

Microtubules respond to FCA and modulate FCA signalling.

Since microtubules re-organise during defence and since microtubule-directed compounds can modify defence responses (Chang and Nick, 2012), we studied the effect of FCA on microtubules in Vrup-TuB6 cells. FCA eliminated cortical microtubules within 30 min **(Fig. 7 b, f, h)**. This does not necessarily imply that microtubules participate in FCA signalling, because they might respond in a parallel pathway. To dissect this, we stabilised microtubules first by taxol prior to FCA treatment which significantly reduced the microtubules elimination by FCA **(Fig. 7 b, g, j).** The stabilisation of microtubules against FCA was followed by a modulated FCA response of defence-related transcripts (**Fig. 7c**). While taxol enhanced transcripts for genes driving phytoalexin biosynthesis (*PAL*, *STS27* and *STS47*), and significantly amplified induction of these transcripts by FCA, the pattern for *MC2*, *MC5* and *PR1* transcripts differed qualitatively. Here, taxol alone did not induce these transcripts and it significantly inhibited their induction by FCA. Although taxol stabilised microtubules against FCA, and modulated the gene expression in response to FCA, it could not mitigate the mortality driven by FCA **(Fig. 7d).** However, comparing the mortality to FCA between our marker line *At*TUB6-GFP (overexpressing β-tubulin), to non-transformed *Vitis rupestris* cell lines, showed that overexpression of ß-tubulin reduced mortality in response to FCA, late to about 25%, at 24 h **(Fig. 7e).** This means that ß-tubulin 6 was able to mitigate FCA toxicity.

To test the effect of microtubules elimination on the mortality response to FCA, we incubated Vrup-TuB6 cells with oryzalin. This strongly depolymerised the microtubules within 30 min **(Fig. 7b, h)**. This elimination was seen as well, when the

oryzalin treatment was followed by addition of FCA **(Fig. 7k)** without any significant difference between these conditions. Furthermore, the pre-treatment of oryzalin did not change the mortality response to FCA (**Fig. S7**).

Since tubulin overexpression decreases susceptibility to FCA, while microtubule elimination is enhancing, microtubules act as negative regulators for FCA-dependent mortality.

Actin filaments respond to and modulate FCA signalling.

Since actin filaments are implicated in PCD signalling (for review see Smertenko & Franklin-Tong, 2011; Chang *et al.*, 2015), we used a grapevine actin-marker cell line expressing (*At*FABD2-GFP) to visualise actin filaments responses to FCA. While in control cells (**Fig. 8a**), actin was organised in a subcortical network of fine strands, it had repartitioned from the cortical network to bundled transvacuolar cables 90 min after FCA addition (**Fig. 8c**). This bundling was significant as seen from measuring bundle width, which was significantly higher in FCA-challenged cells over control cells with $P<0.001$ (**Fig. 8e**). To probe whether this actin bundling is necessary for FCA-triggered PCD we eliminated actin strands by Latrunculin B pre-treatment (**Fig. 8b**). This pre-treatment suppressed either the formation of actin cables in response to FCA (**Fig. 8e**) or FCA-dependent mortality to around half the value seen without latrunculin B (**Fig. 8g**). Again, we measured the FCA response of defence-related genes with latrunculin B pretreatment (**Fig. 8f**). Overall, the patterns were similar, but not identical to those seen for taxol pre-treatment (**Fig. 7h**). While both, latrunculin B and taxol amplified the induction of *STS27* and *STS47* by FCA and both suppressed the induction of *MC5*, the two compounds differed in a couple of points: latrunculin B amplified the FCA response of *JAZ1*, while for *PAL* latrunculin B partially mitigated the induction by FCA, while taxol amplified it further. Likewise, Taxol could clearly suppress the induction of *MC2* and *PR1* by FCA, which was not seen for latrunculin B (**Fig. 8f**). The amplification of *STS27* and *STS47* is of particular interest, because the stabilisation of microtubules and the elimination of actin strands have the same effect, indicating antagonistic roles of the two components of the cytoskeleton in processing the signal deployed by FCA.

Overexpression of metacaspases increased cell death triggered by FCA.

In grapevine, defence-related PCD associates with the upregulation of two specific metacaspases, *MC2* and *MC5* (Gong *et al.*, 2019). As FCA induced the transcript levels of these metacaspases genes, we tested whether these metacaspases participate in the cell death driven by FCA. For this purpose, we used two BY-2 cell lines overexpressing these metacaspases from *V. rupestris*. In fact, these lines, MC2ox and MC5ox exhibited a significantly higher mortality in response to FCA, already manifest at the earliest tested time-point, 3 h (**Fig. 9a**). At 6 h, the mortality was tripled (MC2ox) or doubled (MC5ox) comparing to non-transformed WT, consistent with a causal role of these metacaspases in executing the cell-death response to FCA.

Salicylic Acid mediates FCA triggered mortality, MAPK cascades seem to be dispensible.

Salicylic acid (SA) is often implicated in hypersensitive responses. We tested, therefore, how SA interacts with FCA induced cell death as described in **Method. S1**. The pre-treatment of SA prior to addition of FCA significantly increased mortality from 31% to 44% after 6 hrs (**Fig. 9c**). Since this result suggested that SA is amplifying the mortality response to FCA, we conducted a parallel experiment, where the synthesis of SA was blocked by pre-treatment of 25 μM 1-aminobenzotriazole (ABT) an inhibitor of cytochrome P_{450} oxidases interfering with the phenylalanine-dependent branch of salicylic acid biosynthesis through blocking cinnamic acid 4-hydroxylase (Leon *et al.,* 1995). ABT mitigated the mortality induced by FCA, indicative that endogenous salicylic acid is involved in the transduction of the FCA effect (**Fig. 9b).** In contrast to SA, manipulation of MAPK signalling by the specific inhibitor PD98059, blocking basal immunity in grapevine (Chang and Nick, 2012), caused mortality levels if given alone (**Fig. 9c**), but was not able to cause significant changes in the mortality response to FCA indicating a that cell death is triggered independently of MAPK.

Discussion

The current work was motivated by a working model, where the fungus changes from an endophytic lifestyle with slow progression of disease symptoms to necrotrophy culminating later by apoplexy of the host, which implies that the endophyte must perceive and respond to input from the host (**Fig. 1**). Those changes of plant metabolism that can be used by the fungus to assess and predict the future behaviour of its host, can be defined as "surrender signal" that promotes a transition of the fungus to an aggressive state and favours symptom development. Using a cell-based experimental system based on grapevine suspension cells and the virulent fungus model *Neofusicoccum parvum* Bt-67, we identified this " surrender signal" as ferulic acid, a monolignol induced under drought stress (Griesser *et al.*, 2015). Ferulic acid (in contrast to its precursor coumaric acid) triggers the fungal release of a phytotoxin, FCA. Fusicoccin A, secreted by *Fusicoccum amygdali,* was shown to cause severe mortality in sycamore cells (Malerba *et al.*, 2004) and manipulates several cellular responses initiating with the activity of plasma membrane H^+ ATPases, over remodelling of actin filaments till the regulation of defence genes (Malerba *et al.*, 2008; Singh and Roberts, 2004). In the first step, we analysed the mode of action of FCA and could show that this fungal compound acts as a signal evoking PCD in grapevine cells. Thus, FCA release and the host response to this release could result from changes in the chemical communication between the plant and the pathogen upon water stress. As suggested by the model, the fungus would act as latent endophyte as long the vine does not meet severe climate-born stress. Under challenge by drought ferulic acid accumulates, which, according to our working model, is used by the fungus as signal conveying a severe loss of metabolic homeostasis of the host, such that it will shift into necrotrophic phase. Here, this model stimulates the following questions: 1. What renders ferulic acid so specific as surrender signal under drought stress? 2. By what mechanism can ferulic acid trigger the fungal release of FCA? 3. What is the functional context of FCA-triggered PCD? 4. What does this model contribute to a potential therapy against apoplectic breakdown.

By what mechanism can ferulic acid trigger the fungal release of FCA?

The highly potent phytotoxin, FCA, is synthetised by cyclisation of geranylgeranyl diphosphate (GGDP) by an unusual diterpene synthase harbouring a C-terminal

prenyltransferase domain (Toyomasu *et al.*, 2007). In fact, a homologue with ~60% similarity and all the features of this fusicoccadiene synthase can be located in the *N. parvum* genome (UniProt ID R1H2L0). How ferulic acid can trigger the release of FCA is not known. However, it is a potent activator of fungal laccases that help the fungus to forage lignin as carbon source (for review see Piscitelli *et al.*, 2011). Ferulic acid itself is broken down by feruloyl esterase into vanillin, which is taken up through a specific transporter (Shimizu *et al.*, 2005). Feruloyl esterase can bind the coumaric acid, albeit at a 10-fold reduced affinity, however, it can convert coumaric acid only at a 100-fold reduced velocity (Faulds *et al.*, 2005). Thus, the suppressive activity of coumaric acid on phytotoxin secretion might be caused by coumaric acid blocking the active site of feruloyl esterase. The actual inducer of phytotoxin secretion might therefore be vanillin. In fact, this is supported by our observation that vanillic acid, the oxidised derivative of vanillin, accumulates in the most toxic fraction of fungal exudates (**Fig. 3a**). The transporter for the uptake of vanillin has been already described to be transported to the tip of the growing hyphae through the *Spitzenkörper*, which is also controlling key steps in fungal development, such as the transition from invasive growth towards conidia formation (for review see Harris, 2009). This would link the foraging of ferulic acid as food source with developmental switches controlling the aggressive transition during the pathogen lifestyle: from endophytic biotrophy to necrotrophy, later to full apoplexy.

Why ferulic acid could be an efficient surrender signal upon drought stress?

The conceptual model used in this study is based upon chemical signalling (**Fig. 1**). The chain of events leading to the disease outbreak is promoted by drought stress (**Fig. 2a**), culminating in the accumulation of a plant compound that is utilised by the fungus to assert its aggressiveness. In the search for potential plant compounds that might act as such a "surrender signal", we focussed on the phenylpropanoid pathway for two reasons: 1. This pathway gives rise to stilbenes, the major phytoalexins in grapevine. 2. It also gives rise to lignin, the major carbon source for the fungus, and commonly accumulates under drought stress (Tu *et al.*, 2020). This response is probably of adaptive nature since the apposition of this hydrophobic compound to cell wall helps to retain water for the transport in vascular tissue. In our previous study, we could show that the partitioning of the phenylpropanoid pathway between

stilbenes versus lignin decides on the outcome of plant-fungal interaction (Khattab *et al.*, 2021). In fact, we could show that feeding a specific precursor of monolignols, ferulic acid, induced the fungus to release phytotoxins (**Fig. 2d-f**). Interestingly, cinnamic and coumaric acid, situated upstream of ferulic acid in the pathway, were not inducing phytotoxicity. In contrast, they were even downmodulating the innate toxicity of the fungal culture-filtrate (**Fig. 2e**). Since coumaric acid is also the branching point for the stilbene synthesis, a high steady-state level of coumaric acid would report efficient synthesis of stilbenes, and, thus, would report host vigour. The same holds true, less tightly, for cinnamic acid (in fact, cinnamic acid is silencing phytotoxin release as well, albeit less efficiently compared to coumaric acid). The first metabolite committed for monolignols, is is caffeic acid (www.kegg.jp, search vvi, ferulate). Thus, an increase in the steady-state levels of caffeic acid would report a bottleneck in lignin synthesis and, qualify as readout for the fungus to detect a serious host crisis. Interestingly, and unexpectedly, this is not, what we observe: caffeic acid" is quelling phytotoxicity almost as efficiently as its precursor, coumaric acid. The key to this enigma may be the enzyme 4-coumarate ligase (gene VIT_16s0039g02040, protein UniProt F6HEF8), which is very permissive and accepts any phenolic acid as substrate (cinnamic acid, coumaric acid, caffeic acid, ferulic acid, 5-hydroxy ferulic acid (F5H), and even the monolignol sinapic acid, www.kegg.jp) to confer a Coenzym A residue for further metabolisation. Any change in activity of this enzyme would, therefore, result in a complete shut-down of the entire pathway and, thus, is not apt to act as lever to sense changes in stilbene versus lignin partitioning. However, there exists an enzyme, specifically recruiting ferulic acid for monolignol synthesis: the cytochrome P_{450} 84A1 enzyme ferulate-5-hydroxylase (in grapevine present in tandem as gene VIT_03s0038g00500, protein UniProt D7U5I5 and the almost identical gene VIT_03s0038g00550, protein UniProt F6I194). Ferulate-5-hydroxylase is the rate-limiting enzyme for monolignols synthesis and as such strongly regulated (Ruegger *et al.*, 1999). The fact that this enzyme was among the most pertinent candidates during a transcriptomics study either in *Vitis vinifera* infected with *Neofusicoccum parvum* or even in Chinese wild grapes infected with *Plasmopara viticola* (Massonnet *et al.,* 2017; Liu *et al.*, 2019), could indicate that this gene is subject to tight regulation. The rice homologue of F5H is strongly downregulated under drought (tenor.dna.affrc.go.jp, seach Os06g0349700), especially in roots.

Whether this holds true for grapevine as well, is not known, but would represent a testable implication of the surrender signal model.

What is the functional context of FCA-triggered PCD?

Our data introduce the new concept of "surrender signal" into models of plant-pathogen dialogue (**Fig. 10**). While healthy plants accumulate coumaric acid, a precursor of bioactive stilbenes, whose antifungal properties are able to protect the plant, under climate-born stress, drought, the monolignol precursor ferulic acid accumulates, signalling to the fungus that the plant is under severe stress. In response, the fungus will convert ferulic acid into vanillic acid (Shimizu *et al.*, 2005), which might trigger the transition to sexual development and necrotrophy (culminating in apoplexy) through secretion of phytotoxins, such as FCA, to kill the host and to allow to complete *N. parvum* lifecycle **(Fig. 10. ①, ②)**. After binding to 14-3-3 proteins **(Fig. 10, ③)**, FCA triggers extracellular acidification via binding to PM ATPases in a few minutes (Kinoshita and Shimazaki, 2001: **Fig. 10, ④**), which could trigger cell wall loosening enzymes supporting cell-wall degradation (Kesten et al., 2019). The acidification will also activate RbOH (Huang et al., 2014; Majumdar & Kar, 2018) after 10 min reaching the peak after 60 min (**Fig. 10, ⑤**). Here, superoxide O_2^- acts as upstream signal to trigger FCA stress signalling, since blocking RboH by DPI reduced the FCA-dependant PCD, similar to earlier observations in sycamore cells (Malerba *et al*., 2008). This is followed by microtubule breakdown from 30 min of FCA treatment (**Fig. 10, ⑥**). Microtubules act as negative regulators of signalling, possibly by tethering metacaspases and/or 14-3-3 proteins (Pignocchi and Doonan, 2011)), similar to their role in self-incompatibility (Poulter et al., 2008). Also metacaspases 5, a central regulator of Hypersensitive Response in grapevine (Gong *et al*., 2019) has been shown to be tethered (and possibly restrained) on microtubules Zhu (2020). The breakdown of microtubules might unleash the executors of cell death. If so, taxol pretreatment would be predicted to mitigate cell death. This is not, what we observe (**Fig. 7D**). Alternatively, microtubules, through their amplifying activity in the opening of calcium influx channels might repress PCD indirectly by promoting basal immunity (Nick *et al.*, 2021). Subsequently, from 90 min of FCA treatment, also actin is responding by strong remodelling (**Fig. 10, ⑦**). While actin remodelling accompanies PCD in many systems (Smertenko and Tong, 2011), it does not induce

PCD *per se*. It might be the recruitment of 14-3-3 proteins for the PM ATPases that releases the metacaspases too. In fact, overexpression of type-II metacaspases in poplar is reducing the abundance of 14-3-3 proteins, indicative of a functional interaction (Bollhöner *et al*., 2018). Activation of metacaspases might then trigger expression of metacaspases genes (**Fig. 10, ⑧**) sustaining PCD execution (Tsiatsiani *et al*., 2011; **Fig. 10, ⑨**). Nevertheless, FCA-triggered cell death was independent from MAPK cascades, which were found to be linked to PAMP triggered immunity (PTI) rather than to PCD in grapevine cells (Duan et al., 2016). By contrast, manipulating SA signalling which is more linked to effector triggered immunity (ETI) (Armijo et al., 2013), altered FCA toxicity meaning that FCA signalling would target directly the PCD. Interestingly, most pharmacological treatments mitigating FCA toxicity reduced the accumulated transcripts of genes regulating SA signalling, *PAL* and *PR1*, and increased the transcripts of a competitive pathway *STS27* and *STS47*. Here, we arrived to a conclusion that the phenylpropanoid pathway might act as a lever for the FCA disturbing actions. Several, partially non-intuitive, implications of this model have been tested and confirmed. A rapid oxidative burst, inhibition of the responses by DPI, (destabilising actin) by Latrunculin and (stabilisting microtubules) by taxol, but also the reduced mortality in cells overexpressing GFP-tagged tubulin.

Outlook: What does this model contribute to a potential therapy against Botryosphaeria dieback.

The outputs of this study pave the way for sustainable applications to control Grapevine Trunk Disease by preventing the pathogen to hijack the derivatives of phenylpropanoid pathway to ensure its own aggressiveness. Of course, it will be necessary to validate the phenomena seen in cell cultures also *in planta*, for instance by assessing the correlation between ferulic acid under drought and apoplexy, or to quantify FCA in infected vines. However, already at this stage, the concepts and findings developed in this study stimulate hypothesis-driven application. At least two approaches can be conceived; (i) Chemical genetics as immediate strategy to contain disease outbreak to bridge the time until new resistant varieties become available. In this approach, compound libraries (van de Wouwer et al., 2016) will be used to modulate the pathway to avoid the accumulation of ferulic acid. (ii) Marker-assisted breeding based on genome sequencing of the almost entire population for the

ancestral European Wild Grapevine (Liang et al., 2019), which contain spread of GTDs (Khattab et al., 2021).

Acknowledgement

References

Akaberi S, Wang H, Claudel P, Riemann M, Hause B, Hugueney P, Nick P (2018) Grapevine Fatty Acid Hydroperoxide Lyase Generates Actin-Disrupting Volatiles and Promotes Defence-Related Cell Death. *Journal of Experimental Botany*, 69, 2883–2896.

Andolfi A, Mugnai L, Luque J, Surico G, Cimmino A, & Evidente A (2011) Phytotoxins produced by fungi associated with grapevine trunk diseases. *Toxins* (Vol. 3). https://doi.org/10.3390/toxins3121569

Armijo G, Salinas P, Monteoliva MI, Seguel A, García C, Villarroel-Candia E, Song W, Van der Krol AR, Alvarez Me, Holuigue L (2013) A salicylic acid-induced lectin-like protein plays a positive role in the effector-triggered immunity response of arabidopsis thaliana to pseudomonas syringae Avr-Rpm1. *Molecular Plant-Microbe Interactions*, 26(12), 1395–1406. https://doi.org/10.1094/MPMI-02-13-0044-R

Bollhöner B, Jokipii-Lukkari S, Bygdell J, Stael S, Adriasola M, Muñiz L, Breusegen F. V, Ezcurra I, Wingsle G, Tuominen H (2018) The function of two type II metacaspases in woody tissues of Populus trees. *New Phytologist*, 217(4), 1551–1565.

Bortolami G, Gambetta GA, Delzon S, Lamarque LJ, Pouzoulet J, Badel E, Burlett R, Charrier G, Cochard H, Dayer S, Jansen S (2019) Exploring the Hydraulic Failure Hypothesis of Esca Leaf Symptom Formation 1. *Plant Physiology*, 181(11), 1163–1174.

Buckel I, Andernach L, Schüffler A, Piepenbring M, Opatz T, Thines E (2017) Phytotoxic dioxolanones are potential virulence factors in the infection process of Guignardia bidwellii. *Scientific Reports*, 7(1), 8926.

Byczkowska A, Kunikowska A, Kaźmierczak A (2013) Determination of ACC-induced cell-programmed death in roots of Vicia faba ssp. minor seedlings by acridine orange and ethidium bromide staining. *Protoplasma*, 250(1), 121–128.

Carlucci A, Cibelli F, Lops F, Raimondo ML (2015) Characterization of Botryosphaeriaceae Species as Causal Agents of Trunk Diseases on Grapevines. *Plant Disease*, 99(12), 1678–1688.

Chang X, Heene E, Qiao F, Nick P (2011) The phytoalexin resveratrol regulates the initiation of hypersensitive cell death in vitis cell. *PLoS ONE*, 6(10).

Chang X, Nick P (2012) Defence signalling triggered by Flg22 and Harpin is integrated into a different stilbene output in Vitis cells. *PLoS ONE*, 7(7).

Chang X, Riemann M, Liu Q, Nick P (2015) Actin as deathly switch? How auxin can suppress cell-death related defence. *PLoS ONE*, 10(5), 1–22.

Claverie M, Notaro M, Fontaine F Wery J (2020) Current knowledge on Grapevine Trunk Diseases with complex etiology: A systemic approach. *Phytopathol. Mediterr*, *59*, pp.29-53.

Delaye L., García-Guzmán G., Heil M (2013) Endophytes versus biotrophic and necrotrophic pathogens-are fungal lifestyles evolutionarily stable traits? *Fungal Diversity*, *60*(1), 125–135. https://doi.org/10.1007/s13225-013-0240-y

Duan D, Fischer S, Merz P, Bogs J, Riemann M, Nick P (2016) An ancestral allele of grapevine transcription factor MYB14 promotes plant defence. *Journal of Experimental Botany*, *67*(6), 1795–1804. https://doi.org/10.1093/jxb/erv569

Djoukeng JD, Polli S, Larignon P, Abou-Mansour E (2009) Identification of phytotoxins from Botryosphaeria obtusa, a pathogen of black dead arm disease of grapevine. *European Journal of Plant Pathology*, 124(2), 303–308.

Faulds CB, Molina R, Gonzalez R, Husband F, Juge N, Sanz-Aparicio J,

Hermoso JA. (2005) Probing the determinants of substrate specificity of a feruloyl esterase, AnFaeA, from Aspergillus niger. *FEBS Journal*, 272(17), 4362–4371.

Flubacher, N. S. (2021). 4-Hydroxyphenylacetic acid - a fungal polyketide suppressing plant defence. Dissertation, Karlsruhe Institute of Technology, Germany.

Gaff D, O. Okong'o-Ogola (1971) The use of non-permeating pigments for testing the survival of cells. *Journal of Experimental Botany*. 22:756-758.

Galarneau ERA, Lawrence DP, Travadon R, Baumgartner K (2019) Drought exacerbates botryosphaeria dieback symptoms in grapevines and confounds host-based molecular markers of infection by neofusicoccum parvum. *Plant Disease*, 103(7), 1738–1745.

Gong P, Riemann M, Dong D, Stoeffler N, Gross B, Markel A, Nick P (2019) Two grapevine metacaspase genes mediate ETI-like cell death in grapevine defence against infection of Plasmopara viticola. *Protoplasma*, 256(4), 951–969.

Griesser M, Weingart G, Schoedl-Hummel K, Neumann N, Becker M, Varmuza K, Liebner F, Schuhmacher R, Forneck A (2015) Severe drought stress is affecting selected primary metabolites, polyphenols, and volatile metabolites in grapevine leaves (Vitis vinifera cv. Pinot noir). *Plant Physiology and Biochemistry*, 88, 17–26.

Guan P, Terigele, Schmidt F, Riemann M, Fischer J, Thines E, Nick P (2020) Hunting modulators of plant defence - the Grapevine Trunk Disease fungus *Eutypa lata* secretes an amplifier for plant basal immunity. *Journal of Experimental Botany,* 71, 3710–3724

Guan PY, Schmidt F, Fischer J, Riemann M, Thines E, Nick P (2022) The fungal elicitor eutypine from Eutypa lata activates basal immunity through its phenolic side chains. *Horticultural Research*, doi.org/10.1093/hr/uhac120

Guan X, Buchholz G, Nick P (2015) Tubulin marker line of grapevine suspension cells as a tool to follow early stress responses. *Journal of Plant Physiology*, 176,

118–128.

Guan X, Essakhi S, Laloue H, Nick P, Bertsch C, Chong J (2016) Mining new resources for grape resistance against Botryosphaeriaceae: A focus on Vitis vinifera subsp. sylvestris. *Plant Pathology*, 65(2), 273–284.

Gómez P, Báidez AG, Ortuño A, Del Río JA (2016) Grapevine xylem response to fungi involved in trunk diseases. *Annals of Applied Biology*, 169(1), 116–124.

Harris SD (2009) The Spitzenkörper: A signalling hub for the control of fungal development? *Molecular Microbiology*, 73(5), 733–736.

Hofstetter V, Buyck B, Croll D, Viret O, Couloux A, Gindro K (2012) What if esca disease of grapevine were not a fungal disease? *Fungal Diversity*, 54(May), 51–67.

Huang AX, She XP, Zhao JL, Zhang YY (2014). Inhibition of ABA-induced stomatal closure by fusicoccin is associated with cytosolic acidification-mediated hydrogen peroxide removal. *Botanical Studies*, *55*(1), 1–11. https://doi.org/10.1186/1999-3110-55-33

Kesten C, Gámez- Arjona,FM, Menna A, Scholl S, Dora S, Huerta AI, Huang H, Tintor N, Kinoshita T, M, Krebs M, Schumacher K, Sánchez- Rodríguez, C. (2019). Pathogen- induced pH changes regulate the growth- defense balance in plants. *The EMBO Journal*, 38(24), 1–20. https://doi.org/10.15252/embj.2019101822

Khattab IM, Sahi VP, Baltenweck R, Maia-Grondard A, Hugueney P, Bieler E, Dürrenberger M, Riemann M, Nick P (2021) Ancestral chemotypes of cultivated grapevine with resistance to Botryosphaeriaceae-related dieback allocate metabolism towards bioactive stilbenes. *New Phytologist*, 229(2), 1133–1146.

Kinoshita T, Shimazaki KI (2001) Analysis of the phosphorylation level in guard-cell plasma membrane H+-ATPase in response to fusicoccin. *Plant and Cell Physiology*, 42(4), 424–432.

Labois C, Wilhelm K, Laloue H, Tarnus C, Bertsch C, Goddard, Chong J (2020). Wood Metabolomic Responses of Wild and Cultivated Grapevine to Infection with Neofusicoccum parvum, a Trunk Disease Pathogen. Metabolites, 10(6), 232. https://doi.org/doi:10.3390/metabo10060232

Leal C, Richet N, Guise JF, Gramaje D, Armengol J, Fontaine F, Trotel-Aziz P (2021). Cultivar Contributes to the Beneficial Effects of Bacillus subtilis PTA-271 and Trichoderma atroviride SC1 to Protect Grapevine Against Neofusicoccum parvum. *Frontiers in Microbiology*, 12(October), 1–17. https://doi.org/10.3389/fmicb.2021.726132

Leon J, Shulaev V, Yalpani N, Lawton MA, Raskint I (1995) Benzoic acid 2-hydroxylase, a soluble oxygenase from tobacco, catalyzes salicylic acid biosynthesis (Nicotiana tabacum/tobacco mosaic virus/cytochrome P450/acquired resistance). *Plant Biology*, 92(October), 10413–10417.

Liang Z, Duan S, Sheng J, Zhu S, Ni X, Shao J, Liu C, Nick P, Du F, Fan P et al (2019) Whole-genome resequencing of 472 Vitis accessions for grapevine diversity and demographic history analyses. *Nature Communications*, 10(1), 1–12.

Lima MRM, Machado AF, Gubler WD (2017) Metabolomic Study of Chardonnay Grapevines Double Stressed with Esca-Associated Fungi and Drought. *Phytopathology*, 107(6), 669–680.

Liu R, Weng K, Dou M, Chen T, Yin X, Li Z, Li T, Zhang C, Xiang G, Liu G et al (2019) Transcriptomic analysis of Chinese wild Vitis pseudoreticulata in response to Plasmopara viticola. *Protoplasma* 256, 1409-1424.

Livak KJ, Schmittgen TD (2001) Analysis of relative gene expression data using real-time quantitative PCR and the 2(−Delta Delta C(T)) method. *Methods* 25, 402–408.

Loeffler F (1884) Untersuchung über die Bedeutung der Mikroorganismen für die Entstehung der Diphtherie beim Menschen, bei der Taube und beim Kalbe. Mittheilungen kaiserl Gesundheitsamt 2, 421–499.

Majumdar A, Kar RK (2018) Congruence between PM H$^+$-ATPase and NADPH oxidase during root growth: a necessary probability. *Protoplasma*. Jul;255(4):1129-1137.

Malerba M, Cerana R, Crosti P (2004). Comparison between the effects of fusicoccin, Tunicamycin, and Brefeldin A on programmed cell death of cultured sycamore (Acer pseudoplatanus L.) cells. *Protoplasma*, 224(1–2), 61–70. https://doi.org/10.1007/s00709-004-0053-7

Malerba M, Contran N, Tonelli M, Crosti P, Cerana R (2008) Role of nitric oxide in actin depolymerization and programmed cell death induced by fusicoccin in sycamore (Acer pseudoplatanus) cultured cells. *Physiologia Plantarum*, 133(2), 449–457.

Massonnet M, Figueroa-Balderas R, Galarneau ERA, Miki S, Lawrence DP, Sun Q, Wallis CM, Baumgartner K, Cantu D (2017) Neofusicoccum parvum Colonization of the Grapevine Woody Stem Triggers Asynchronous Host Responses at the Site of Infection and in the Leaves. *Frontiers in Plant Science*, 8(June).

Mugnai L, Graniti A, Surico G (1999) Esca (Black Measles) and Brown Wood-Streaking: Two Old and Elusive Diseases of Grapevines. *Plant Disease*, 83(5), 404–418.

Nick P, Guan P, Shi WJ, Riemann M (2021) Dissecting the Membrane-Microtubule Sensor in Grapevine Defence. *Horticulture Research*, 8, 260.

Pietrowska E, Różalska S, Kaźmierczak A, Nawrocka J, Małolepsza U (2014) Reactive oxygen and nitrogen (ROS and RNS) species generation and cell death in tomato suspension cultures—Botrytis cinerea interaction. *Protoplasma*, 252(1), 307–319.

Pignocchi C, Doonan JH (2011) Interaction of a 14-3-3 protein with the plant microtubule-associated protein EDE1. *Annals of Botany*, 107(7), 1103–1109.

Piscitelli A, Giardina P, Lettera V, Pezzella C, Sannia G, Faraco V (2011) Induction and transcriptional regulation of laccases in fungi. *Curr Genomics*.

12(2):104-112.

Pitt WM, Huang R, Steel CC, Savocchia S (2013). Pathogenicity and epidemiology of Botryosphaeriaceae species isolated from grapevines in Australia. *Australasian Plant Pathology*, *42*(5), 573–582. https://doi.org/10.1007/s13313-013-0221-3

Poulter NS, Vatovec S, Franklin-Tong VE (2008) Microtubules are a target for self-incompatibility signaling in Papaver pollen. *Plant Physiology*, 146(3), 1358–1367.

Pouzoulet J, Scudiero E, Schiavon M, Rolshausen PE (2017) Xylem vessel diameter affects the compartmentalization of the vascular pathogen Phaeomoniella chlamydospora in grapevine. *Frontiers in Plant Science*, 8, 1–13.

Qiao F, Chang XL, Nick P (2010) The cytoskeleton enhances gene expression in the response to the Harpin elicitor in grapevine. *Journal of Experimental Botany*, 61(14), 4021–4031.

Reis P, Magnin-Robert M, Nascimento T, Spagnolo A, Abou-Mansour E, Fioretti C, Clement C, Rego C, Fontaine F (2016). Reproducing Botryosphaeria dieback foliar symptoms in a simple model system. *Plant Dis*., 100,1071-1079.

Reveglia P, Billones- baaijens R, Niem JM, Masi M, Cimmino A, Evidente A, Savocchia S (2021) Production of phytotoxic metabolites by botryosphaeriaceae in naturally infected and artificially inoculated grapevines. *Plants*, 10(4), 1–17. https://doi.org/10.3390/plants10040802

Ruegger M, Meyer K, Cusumano JC, Chapple C (1999) Regulation of Ferulate-5-Hydroxylase Expression in Arabidopsis in the Context of Sinapate Ester Biosynthesis, *Plant Physiology*, 119: 101-110.

Schwarzerová K, Zelenková S, Nick P, Opatrný Z (2002) Aluminum-induced rapid changes in the microtubular cytoskeleton of tobacco cell lines. *Plant and Cell Physiology*, 43(2), 207–216.

Shimizu M, Kobayashi Y, Tanaka H, Wariishi H (2005) Transportation

mechanism for vanillin uptake through fungal plasma membrane. *Applied Microbiology and Biotechnology*, 68(5), 673–679.

Singh J, Roberts MR (2004) Fusicoccin activates pathogen-responsive gene expression independently of common resistance signalling pathways, but increases disease symptoms in Pseudomonas syringae-infected tomato plants. *Planta*, 219(2), 261–269. https://doi.org/10.1007/s00425-004-1234-5

Slippers B, Wingfield MJ (2007) Botryosphaeriaceae as endophytes and latent pathogens of woody plants: diversity, ecology and impact. *Fungal Biology Reviews*, 21(2–3), 90–106.

Smertenko A, Franklin-Tong VE (2011) Organisation and regulation of the cytoskeleton in plant programmed cell death. *Cell Death and Differentiation*, 18(8), 1263–1270.

Stempien E, Goddard ML, Wilhelm K, Tarnus C, Bertsch C, Chong J (2017) Grapevine Botryosphaeria dieback fungi have specific aggressiveness factor repertory involved in wood decay and stilbene metabolization. *PLoS ONE*, 12(12), 1–22.

Steffens B, Sauter M (2009) Epidermal cell death in rice is confined to cells with a distinct molecular identity and is mediated by ethylene and H2O2 through an autoamplified signal pathway. *Plant Cell*, 21(1), 184–196.

Stevers LM, Sijbesma E, Botta M, Mackintosh C, Obsil T, Landrieu I, Cau Y, Wilson AJ, Karawajczyk V, Eickhoff J et al (2018) Modulators of 14-3-3 Protein-Protein Interactions. *Journal of Medicinal Chemistry*, 61(9), 3755–3778.

Svyatyna, K., Jikumaru, Y., Brendel, R., Reichelt, M., Mithöfer, A., Takano, M., Kamiya Y, Nick P, Riemann, M (2014) Light induces jasmonate-isoleucine conjugation via OsJAR1-dependent and -independent pathways in rice. *Plant, Cell and Environment*, 37(4), 827–839.

Toyomasu T, Tsukahara M, Kaneko A, Niida R, Mitsuhashi W, Dairi T, Kato N, Sassa T (2007) Fusicoccins are biosynthesized by an unusual chimera diterpene synthase in fungi. *Proceedings of the National Academy of Sciences of the*

United States of America, 104(9), 3084–3088.

Trotel-Aziz P, Robert-Siegwald G, Fernandez O, Leal C, Villaume S, Guise J-F, Abou-Mansour E, Lebrun M-H, Fontaine F (2022) Diversity of Neofusicoccum parvum for the Production of the Phytotoxic Metabolites (-)-Terremutin and (R)-Mellein. *Journal of Fungi*, 8(3):319. https://doi.org/10.3390/jof8030319

Tsiatsiani L, Van Breusegem F, Gallois P, Zavialov A, Lam E, Bozhkov PV (2011). Metacaspases. *Cell Death and Differentiation*, *18*(8), 1279–1288. https://doi.org/10.1038/cdd.2011.66

Tu M, Wang X, Yin, W. Yin W, Wang Y, Li Y, Zhang G, Li Z, Song J, Wang X (2020) Grapevine VlbZIP30 improves drought resistance by directly activating VvNAC17 and promoting lignin biosynthesis through the regulation of three peroxidase genes. *Horticultural Research*, 7, 150.

Umezawa T (2010). The cinnamate/monolignol pathway. Phytochemistry Reviews, 9(1), 1–17. https://doi.org/10.1007/s11101-009-9155-3

Úrbez-Torres JR, Gubler WD (2009) Pathogenicity of Botryosphaeriaceae species isolated from grapevine cankers in California. *Plant Disease*, 93(6), 584–592.

Úrbez-Torres JR (2011) The status of Botryosphaeriaceae species infecting grapevines José. *Phytopathologia Mediterranea*, 50(4).

van de Wouwer D, Vanholme R, Decou R, Goeminne G, Audenaert D, Nguyen L, Höfer R, Pesquet E, Vanholme B, Boerjan W (2016) Chemical genetics uncovers novel inhibitors of lignification, including p-iodobenzoic acid targeting CINNAMATE-4-HYDROXYLASE. *Plant Physiology*, 172(1), 198–220.

Wang R, Duan D, Metzger C, Zhu X, Riemann M, Pla M, Nick P (2022) Aluminum can activate grapevine defense through actin remodeling, *Horticulture Research*, 9, 016, https://doi.org/10.1093/hr/uhab016

Watanabe N, Lam E (2011) Arabidopsis metacaspase 2d is a positive mediator of cell death induced during biotic and abiotic stresses. *Plant Journal*, 66(6), 969–

982.

Zhu X (2020) Green leaf volatile Triggered Defense Signalling and Cell Death Mediated by Vitis Metacaspase 5. PhD thesis. Karlsruhe Institute of Technology, Germany.

Fig. 1. Working model on host-pathogen interaction during Vitis-Botryosphaeriaceae Dieback used to structure the current study. After entry through pruning wounds, the fungus first colonises wood fibres and xylem parenchyma and follows an endophytic lifestyle, to a certain extent also showing a transition of necrotrophy at a low level, which is contained by a local and mild defence response of the host (accumulation of phenolic compounds). Host defence is partially quelled by immunity-suppressing signals secreted by the endophyte in a tug-of-war. This pre-critical phase can last for years and under favourable conditions will not impair productivity nor vigour of the host. However, if the host is shifted under severe stress such as heat or drought, the critical phase can be initiated. Here, the stress-dependent, chronic loss of physiological homeostasis of the host results in molecular changes that can be perceived by the fungus as surrender signals and activate the transition to apoplexy. This critical phase is, therefore, followed by a terminal phase, where the fungus is producing phytotoxins and initiates sporulation and formation of fruiting bodies resulting in the death of the host and the spread of spores that can colonise neighbouring vines.

Fig. 2. Shifting the fungal strain, *Neofusicoccum parvum* Bt-67, to necrotrophic lifestyle. **a-c)** Effect of drought stress on fungal development *in planta*. **a)** representative grapevines (*V. vinifera* cv. Augster Weiß) raised under either control conditions (optimal water regime) or drought stress (20% of optimal water regime), **b** coverage of wood necrosis in plants that have been wounded and mock inoculated (W) versus plants infected with *Neofusicoccum parvum* Bt-67 (NP) one-month after inoculation, **c)** lignin content at the inoculation site in mock inoculated versus infected canes one month after inoculation. **d)** Monolignol pathway showing the positions of cinnamic acid (CINN), *p*-coumaric acid (COUM), caffeic acid (CAFF), and ferulic acid (FER). **e)** Experimental design to screen for the surrender signal. Candidate monolignols are fed to *N. parvum* (NP) and the culture filtrate is collected after 2 weeks and added to *V. rupestris* GFP-TuB6 as recipient to screen for phytotoxicity **(c)** Mortality of the recipient cells scored in response to culture filtrate from *N. parvum* after feeding the fungal donor with different monolignols as compared to culture filtrate from mock-treated cells (NP), or without any filtrate (CTRL). **f)** Mortality of the recipient cells in response to fungal metabolites extracted from mycelia (MYC) or recovered from the culture filtrates (CF) after fermentation for 24 hr with *p*-coumaric acid or ferulic acid to probe for potential differences in the secretion of the phytotoxins. Data represent means and SE from three independent biological experiments. Asterisks indicate statistical differences by LSD test at significance level with $P<0.05$ (*), $P<0.01$ (**). and $P<0.001$ (***) in **b)** and **c)**. Different letters

represent statistical differences based on Duncan's test with significant levels $P<0.05$ in **e)** and **f).**

Fig. 3. Identifying the fungal toxin released in response to fermentation with ferulic acid for 24 hr. **a)** HPLC UV readouts for the fungal metabolites secreted by *Neofusicocum parvum* Bt-67 in response to fermentation with 0.5 mM ferulic acid and fractionated using a solid phase extraction with a gradient of acetonitrile (0-100% MeCN). **b)** Mortality of *Vitis rupestris* GFP-TuB6 suspension cells in response to the fractions from fungal culture filtrates shown in **a)**. For each fraction, a concentration of 20 µg/ml *Vitis* cells was administered. **c)** Correlation between mortality of the *Vitis* recipient cells and the area for the peak highlighted in **a)** by the red box . **d)** Mortality of *V. rupestris* GFP-TuB6 cells in response to subfractions obtained from the most hydrophobic fraction of the acetonitrile gradient (MeCN 100%) of *N. parvum* fermented with ferulic acid. Here, a lower concentration (13.3 µg/ml Vitis cells was used, as compared to b), because the subfractions were more efficient and the material had to be safeguarded for structural elucidation. Mortality was scored after 24 h. **e)** Compound isolated from the fraction B1 by LC-MS analysis and identified as a derivative of Fusicoccin A. Bars represent means and SE from three independent experimental series. Asterisks indicate statistical differences by LSD test at significance level with $P<0.05$ (*), $P<0.01$ (**). and $P<0.001$ (***) in **b)**. Different letters represent statistical differences based on Duncan's test with significant levels $P<0.05$ in **d)**.

Fig 4. Cytological characterisation of the cell death in *Vitis* cells in response to Fusicoccin A. The cell death response was classified based on double staining with the membrane-permeable fluorochrome Acridine Orange (green signal) and the membrane-impermeable fluorochrome Ethidium Bromide (red signal). Living cells exclude Ethidium Bromide and appear green, cells in stage 1 show penetration of Ethidium Bromide into the cytoplasm, but still exclude the dye from the karyoplasm, cells in stage 2 show penetration of Ethidium Bromide into the nucleus, dead cells loose the Acridine Orange signal due to complete breakdown of the plasma membrane, while Ethidium Bromide remains sequestered at the DNA. Frequency of either living, dying or dead cells was calculated based on their fluorescence intensity values (FI) according to the provided colour scale. Time course of these stages in response to 6 µM **(a)** and 12 µM **(b)** Fusicoccin A. Frequency distributions represent 300-400 individual cells collected from three independent experimental series. **(c-f)** progressive stages of autolytic cell death induced by Fusicoccin A, such as chromatin condensation in interphase nuclei (c, chrom), or appearance of lytic vacuoles (lv) in the cytoplasm (d, e). A dead cell void of cytoplasmic signals, but nuclei (nu) labelled by Ethidium Bromide, representing the terminal stage, is shown in **(f)**.

Fig 5. Rapid responses of *V. rupestris* GFP-TuB6 cells to Fusicoccin A (FCA). **a)** Activation of plasma-membrane proton ATPases by Fusicoccin A (6 µM) as detected by acidification of the extracellular medium. **b)** Detection of superoxide anions by 0.1% Nitroblue Tetrazolium. Data represent a population of 600-700 stained cells from three independent experimental series**. c)** Modulation of steady-state transcript levels of stress-marker genes measured by qPCR in response to Fusococcin A (6 µM)

showing steady-state levels for transcripts involved in cell-death signalling such as mitochondrial (*MnSOD*) and plastidic (*CuSOD*) superoxide dismutase genes, as well as defence-related metacaspaces (*MC2, MC5*) over time. **d)** Transcripts of the phenyl propanoid pathway initiating from phenylammonium lyase (*PAL*), exemplarily probing monolignol synthesis (*CAOMT*, *CAD*) and stilbene synthesis (*STS6*, *STS16*, *STS27*, *STS47*). **e)** Transcripts of phytohormonal signalling genes (*JAZ1, JAZ2, JAZ9* for jasmonates; *PR1, ICS* for salicylic acid). Colour code represents the significant fold changes of 3 biological replicates normalised to the control of the respective time-point. Different letters represent statistical differences based on Duncan's test with significant levels *P*<0.05.

Fig. 6. Role of 14-3-3 proteins **(a-d)** and Respiratory burst oxygen Homologue (RbOH, **e-h**) for the cellular responses to Fusicoccin A. **a, e)** Working model of FCA-signalling used to structure the experiments. Response of extracellular acidification as readout for plasma-membrane localised proton ATPases **(b)**, specific defence related transcripts **(c),** and cell death **(d)** to either 6 μM Fusicoccin A (FCA) alone or following a pre-treatment with 5 μM of the 14-3-3 inhibitor BV02 for 30 min. As negative control, BV02 was also tested without subsequent addition of FCA. Response of superoxide production as readout for RboH **(f)**, specific defence related transcripts **(g),** and cell death **(h)** to either 6 μM Fusicoccin A (FCA) alone or following a pre-treatment with 1 μM of the RboH inhibitor DPI for 60 min. Data represents mean and SE from 3 independent biological replicates. Asterisks indicate statistical differences by LSD test at significance level with *P*<0.05 (*), *P*<0.01 (**). and *P*<0.001 (***).
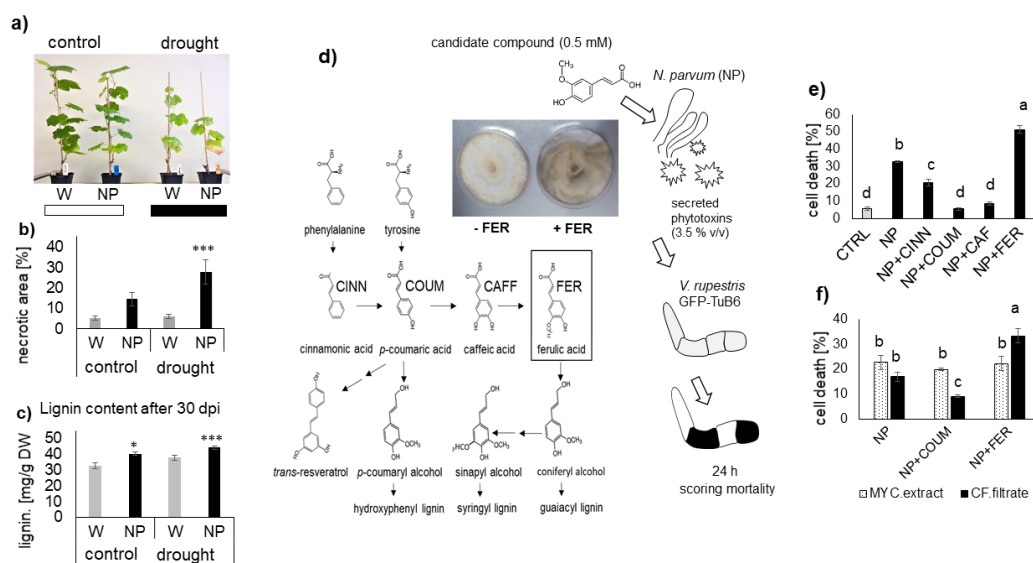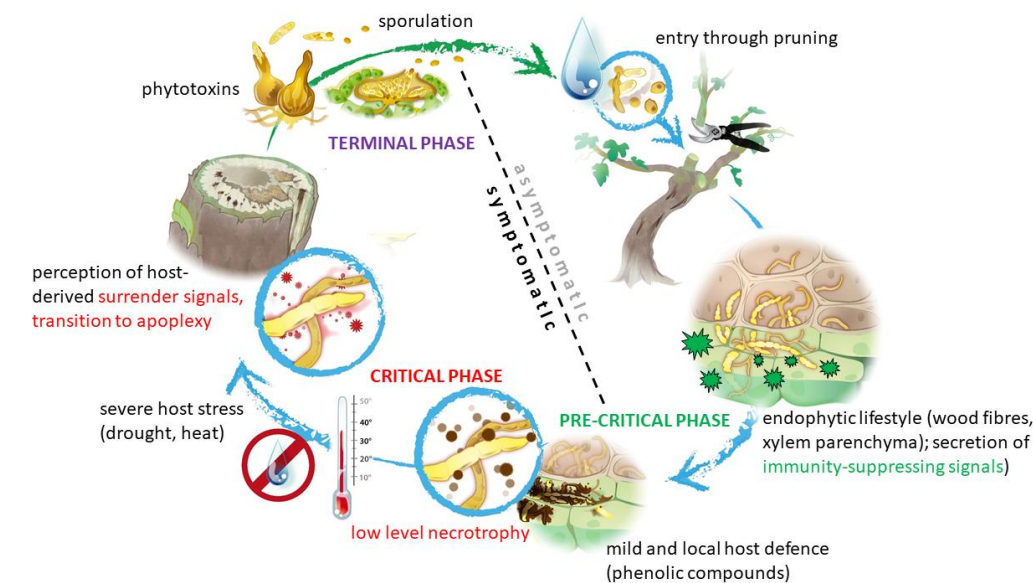
Fig. 7. Microtubular response to Fusicoccin A, and role of microtubules for the cellular responses to Fusicoccin A. **a)** Working model of FCA-signalling used to structure the experiments. **b)** Quantification of microtubule integrity for the treatments shown representatively in **(f-k)**. Data represent medians, inter-quartiles, and extreme values for measurements from at least 30 individual cells. **c)** Heat map of steady-state transcripts levels for specific defence genes 1 h after addition of 6 μM FCA either alone or in combination with 10 μM Taxol . **d)** Mortality scored at 6 h after addition of either 6 μM FCA, 10 μM Taxol, or a combination of both compounds. **e)** Overexpression of microtubules in the *Vitis rupestris* cell line *At*TUB6-GFP mitigates mortality in response to Fusicoccin A comparing to non-transformed *Vitis rupestris* wild type. Representative *V. rupestris* GFP-TuB6 cells after 30 min of treatment with microtubule-modulating compounds either in the absence **(f-h)** or in presence of FCA **(d-f)**. Solvent controls **(i-k)** 0.1% DMSO, 10 μM taxol **(b, e)**, or 10 μM Oryzalin **(c, f)** are shown. Data represent mean and standard errors from three independent biological experiments comprising 1500 individual cells. Different letters represent statistical differences based on Duncan's test with significant levels *P*<0.05 in **b)** and **e)**. Asterisks indicate statistical differences by LSD test at significance level with *P*<0.05 (*), *P*<0.01 (**). and *P*<0.001 (***) in **c)** and **d).**
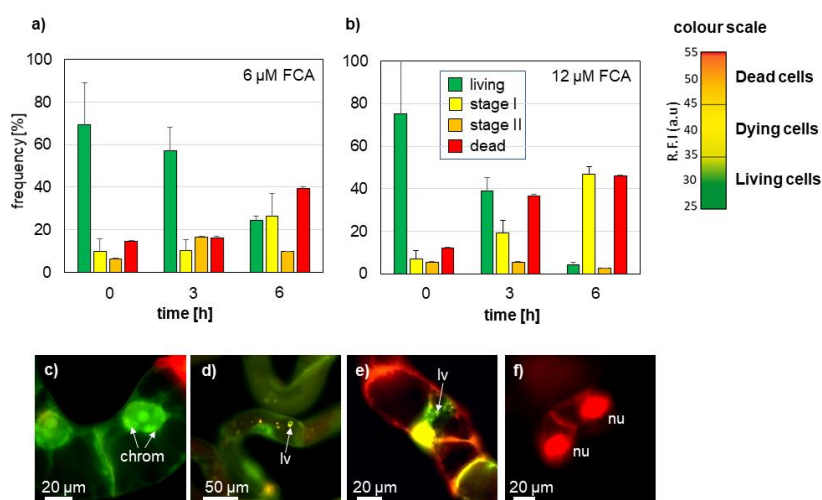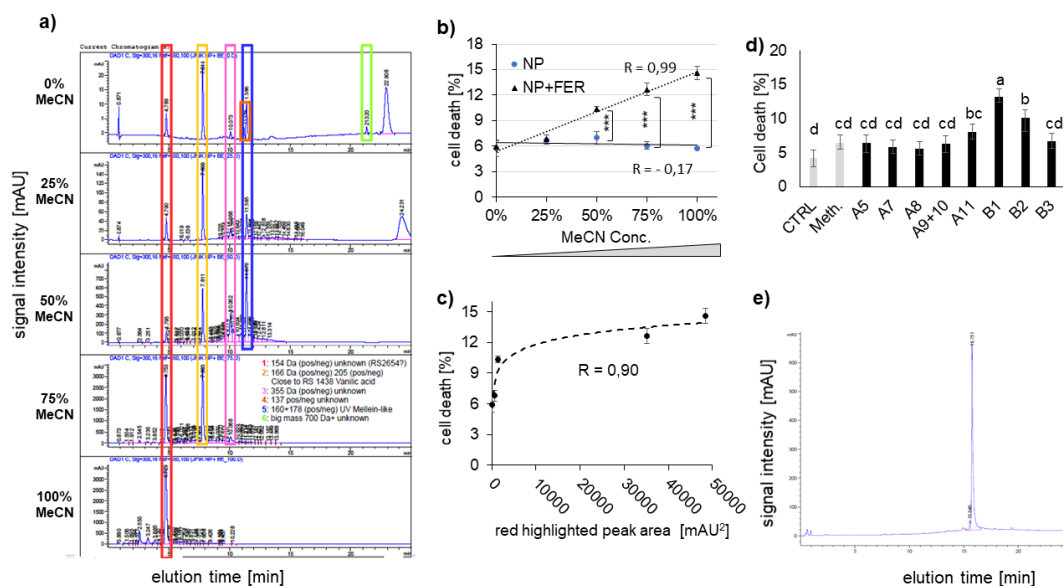
Fig. 8. Actin response to Fusicoccin A, and role of actin for the cellular responses to Fusicoccin A (6 μM). **a)** Working model of FCA-signalling used to structure the

experiments. **b)** quantification of actin bundling for the treatments shown representatively in **(e-h)**. Data represent medians, quartiles, and extreme values for measurements from at least 30 individual cells. **c)** heat map of steady-state transcripts levels of stress-marker genes 1 h after addition of 6 µM FCA either alone or in combination with 2 µM LatB .**d)** Mortality scored at 6 h after addition of either 6 µM FCA, 2 µM FCA, or a combination of both compounds. Representative *V. vinifera* cv. Chardonnay FABD2-GFP cells after 90 min of treatment with the actin-eliminating compound Latrunculin B (2 µM) in the absence **(f)** or in presence of FCA **(h)**, compared to the solvent control **(e)** 0.1% DMSO, or to Fusicoccin A alone **(g)**. Data represent mean and standard errors from three independent biological experiments comprising 1500 individual cells. Asterisks indicate statistical differences based on LSD test with significant levels *P*<0.05 (*), *P*<0.01 (**), and *P*<0.001 (***).

Fig. 9. Probing for molecular components of the FCA response. **(a)** Role of metacaspases. Time course of cell death in response to 6 µM Fusicoccin A in non transformed tobacco BY-2 cells (WT), and in cells overexpressing either metacaspase 2 (MC2ox) or metacaspase 5 (MC5ox) from *Vitis rupestris*. **(b)** Role of salicylic acid (SA, 50 µM) and its inhibitor, 1-aminobenzotriazole (ABT, 25 µM) scored 6 h after addition of 6 µM Fusicoccin A in *V. rupestris* GFP-TuB6 cells. **(c)** Role of MAPK signalling. Cell death scored 6 h after addition of 6 µM Fusicoccin A to *Vitis rupestris* GFP-TuB6 cells following pre-treatment with 50 µM of the MAPK inhibitor PD98059 for 60 min. Data represent means and SE from 3 biological replicates comprising 1500 individual cells per data point. Different letters represent statistical differences based on Duncan's test with significant levels P<0.05 **(a)**, asterisks indicate statistical differences based on LSD test with significant levels P<0.05 (*), P<0.01 (**), and P<0.001 (***) in **b)** and **c)**.

Fig. 10. Working model showing the chemical communication driving apoplexy in Botryosphaeria-ceae-*Vitis* interaction and the stress signalling induced by the apoplexy signal (Fusicoccin A).
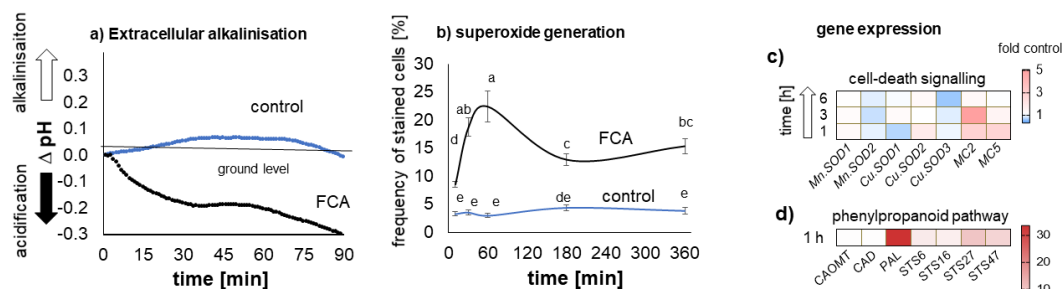
Fig 5. Rapid responses of *V. rupestris* GFP-TuB6 cells to Fusicoccin A (FCA). **a)** Activation of plasma-membrane proton ATPases by Fusicoccin A (6 μM) as detected by acidification of the extracellular medium. **b)** Detection of superoxide anions by 0.1% Nitroblue Tetrazolium. Data represent a population of 600-700 stained cells from three independent experimental series**. c)** Modulation of steady-state transcript levels of stress-marker genes measured by qPCR in response to Fusococcin A (6 μM) showing steady-state levels for transcripts involved in cell-death signalling such as mitochondrial (*MnSOD*) and plastidic (*CuSOD*) superoxide dismutase genes, as well as defence-related metacaspaces (*MC2, MC5*) over time. **d)** Transcripts of the phenyl propanoid pathway initiating from phenylammonium lyase (*PAL*), exemplarily probing monolignol synthesis (*CAOMT, CAD*) and stilbene synthesis (*STS6, STS16, STS27, STS47*). **e)** Transcripts of phytohormonal signalling genes (*JAZ1, JAZ2, JAZ9* for jasmonates; *PR1, ICS* for salicylic acid). Colour code represents the significant fold changes of 3 biological replicates normalised to the control of the respective time-point. Different letters represent statistical differences based on Duncan's test with significant levels *P*<0.05.
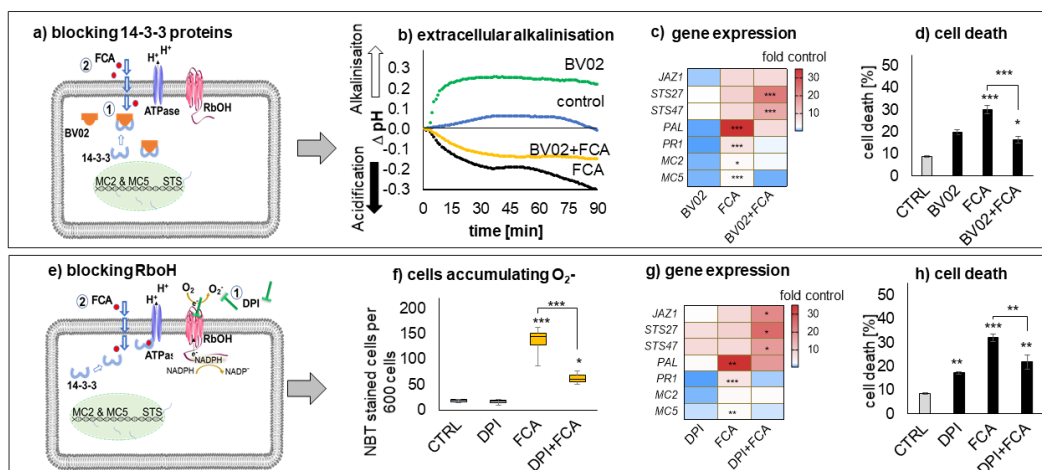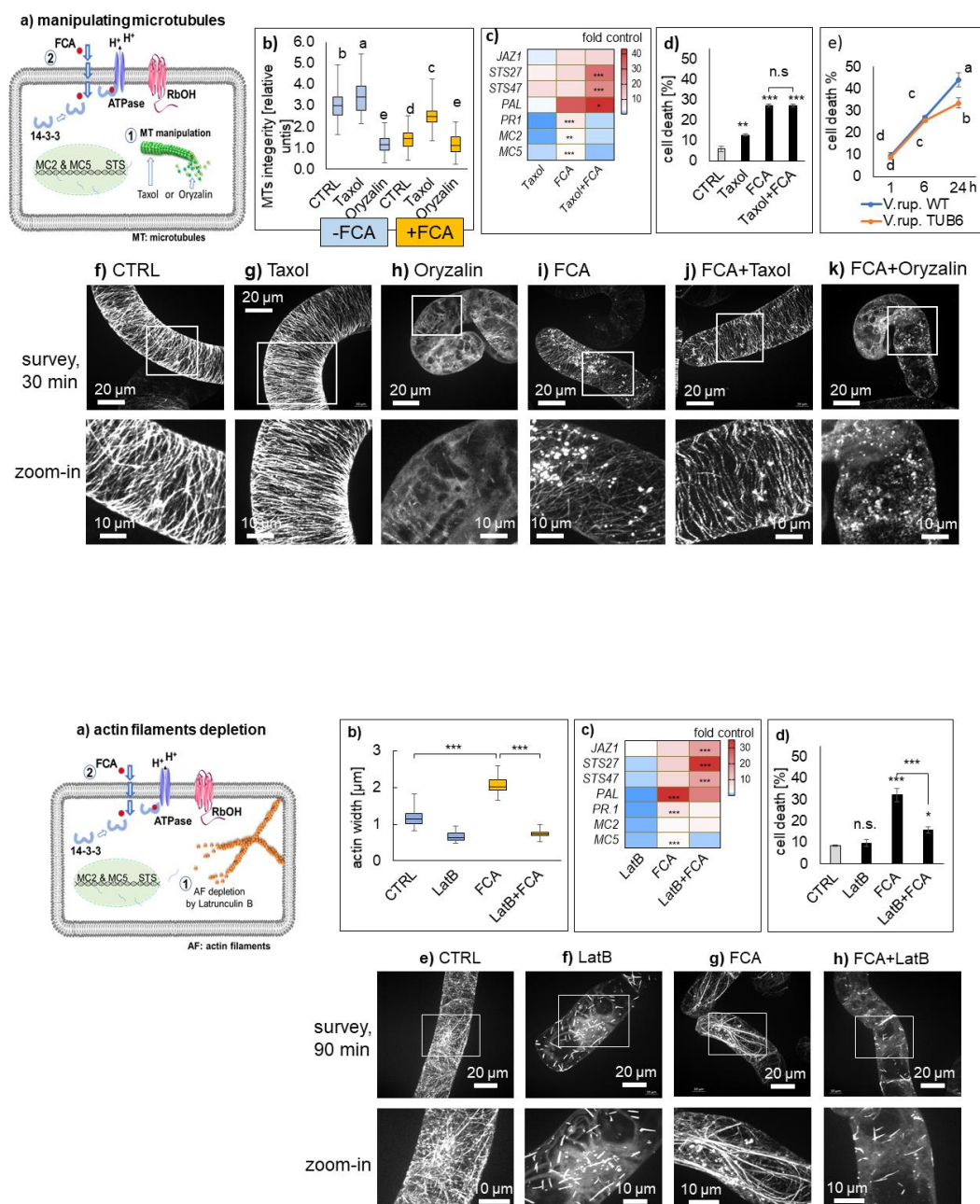

Fig. 6. Role of 14-3-3 proteins (**a-d**) and Respiratory burst oxygen Homologue (RbOH, **e-h**) for the cellular responses to Fusicoccin A. **a, e**) Working model of FCA-signalling used to structure the experiments. Response of extracellular acidification as readout for plasma-membrane localised proton ATPases (**b**), specific defence related transcripts (**c**), and cell death (**d**) to either 6 μM Fusicoccin A (FCA) alone or following a pre-treatment with 5 μM of the 14-3-3 inhibitor BV02 for 30 min. As negative control, BV02 was also tested without subsequent addition of FCA. Response of superoxide production as readout for RboH (**f**), specific defence related transcripts (**g**), and cell death (**h**) to either 6 μM Fusicoccin A (FCA) alone or following a pre-treatment with 1 μM of the RboH inhibitor DPI for 60 min. Data represents mean and SE from 3 independent biological replicates. Asterisks indicate statistical differences by LSD test at significance level with *P*<0.05 (*), *P*<0.01 (**). and *P*<0.001 (***).

a) manipulating microtubules

b) MTs integrity [relative units]

c) fold control

d) cell death [%]

e) cell death %

V.rup. WT
V.rup. TUB6

f) CTRL **g)** Taxol **h)** Oryzalin **i)** FCA **j)** FCA+Taxol **k)** FCA+Oryzalin

survey, 30 min

zoom-in

a) actin filaments depletion

b) actin width [μm]

c) fold control

d) cell death [%]

e) CTRL **f)** LatB **g)** FCA **h)** FCA+LatB
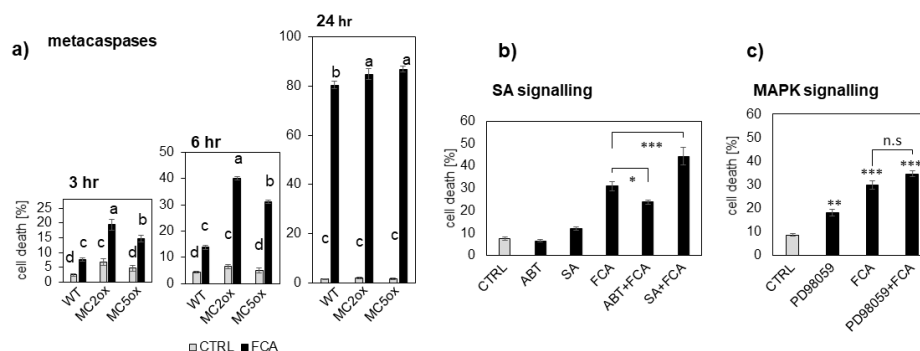
survey, 90 min

zoom-in

Fig. 9. Probing for molecular components of the FCA response. **(a)** Role of metacaspases. Time course of cell death in response to 6 μM Fusicoccin A in non transformed tobacco BY-2 cells (WT), and in cells overexpressing either metacaspase 2 (MC2ox) or metacaspase 5 (MC5ox) from *Vitis rupestris*. **(b)** Role of salicylic acid (SA, 50 μM) and its inhibitor, 1-aminobenzotriazole (ABT, 25 μM) scored 6 h after addition of 6 μM Fusicoccin A in *V. rupestris* GFP-TuB6 cells. **(c)** Role of MAPK signalling. Cell death scored 6 h after addition of 6 μM Fusicoccin A to *Vitis rupestris* GFP-TuB6 cells following pre-treatment with 50 μM of the MAPK inhibitor PD98059 for 60 min. Data represent means and SE from 3 biological replicates comprising 1500 individual cells per data point. Different letters represent statistical differences based on Duncan's test with significant levels P<0.05 **(a)**, asterisks indicate statistical differences based on LSD test with significant levels P<0.05 (*), P<0.01 (**), and P<0.001 (***) in **b)** and **c)**.

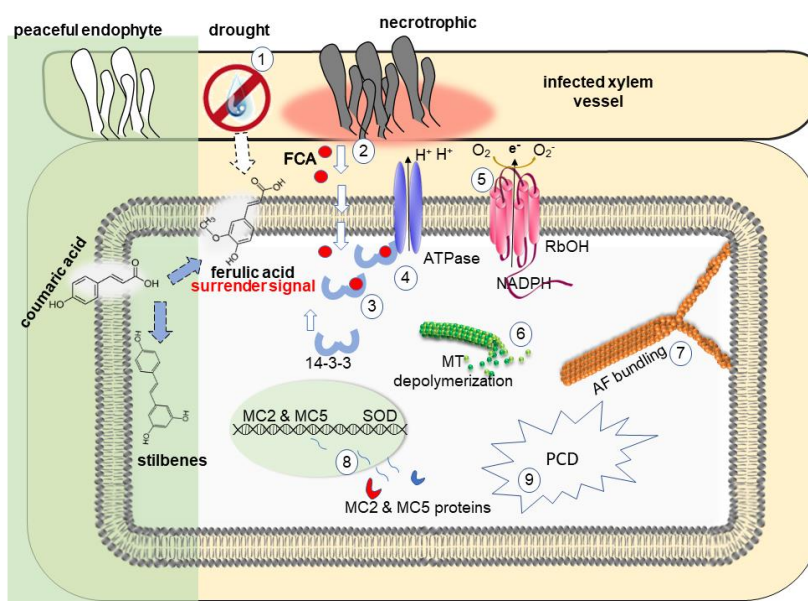**Fig. 10.** Working model showing the chemical communication driving apoplexy in Botryosphaeria-ceae-*Vitis* interaction and the stress signalling induced by the apoplexy signal (Fusicoccin A)